

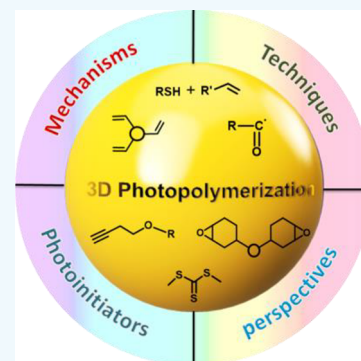
Photopolymerization in 3D Printing

Ali Bagheri*¹ and Jianyong Jin*¹

School of Chemical Sciences, The University of Auckland, Auckland 1010, New Zealand

ABSTRACT: The field of 3D printing is continuing its rapid development in both academic and industrial research environments. The development of 3D printing technologies has opened new implementations in rapid prototyping, tooling, dentistry, microfluidics, biomedical devices, tissue engineering, drug delivery, etc. Among different 3D printing techniques, photopolymerization-based process (such as stereolithography and digital light processing) offers flexibility over the final properties of the 3D printed materials (such as optical, chemical, and mechanical properties) using versatile polymer chemistry. The strategy behind the 3D photopolymerization is based on using monomers/oligomers in liquid state (in the presence of photoinitiators) that can be photopolymerized (via radical or cationic mechanism) upon exposure to light source of different wavelengths (depending on the photoinitiator system). An overview of recent evolutions in the field of photopolymerization-based 3D printing and highlights of novel 3D printable photopolymers is provided herein. Challenges that limit the use of conventional photopolymers (i.e., initiation under UV light) together with prospective solutions such as incorporation of photosensitive initiators with red-shifted absorptions are also discussed in detail. This review also spotlights recent progress on the use of controlled living radical photopolymerization techniques (i.e., reversible addition–fragmentation chain-transfer polymerization) in 3D printing, which will pave the way for widespread growth of new generations of 3D materials with living features and possibility for postprinting modifications.

KEYWORDS: 3D printing, photopolymerization, UV light-sensitive photoinitiators, visible light-sensitive photoinitiators, photopolymerization mechanisms, controlled living radical polymerization



1. INTRODUCTION

3D printing techniques (otherwise known as additive manufacturing, rapid prototyping, or layered manufacturing) were introduced during the 1980s with the aim to fabricate customized/complex objects without the need for molds or machining.^{1,2} Due to the versatile polymer chemistry-related innovations, photopolymerization-based 3D printing techniques have attracted special attention from polymer chemists, material scientists, and engineers.^{3,4} 3D photopolymerization-based techniques such as stereolithography (SLA), digital light processing (DLP), and continuous liquid interface production (CLIP) enable 3D fabrication of complex multifunctional material systems with controllable optical, chemical, and mechanical properties.^{3,5} High resolution with low feature size (in the range of micrometer) is also achievable using these techniques.⁶ To this end, this technology has opened new directions in various fields such as microfluidics, biomedical devices, soft robotics, surgery, tissue engineering, dentistry, and drug delivery.^{7–9}

The strategy behind the 3D photopolymerization (also known as photocuring or photo-cross-linking) is based on using monomers/oligomers in a liquid state that can be cured/photopolymerized upon exposure to light source of specific wavelength and form thermosets.¹⁰ A photoinitiator or photoinitiator system (with relatively high absorption coefficients) is required to convert photolytic energy into the reactive species (radical or cation) which can drive the chain growth via radical or cationic mechanism. Typically, photo-

initiators with high molar extinction coefficients at short wavelength (mostly UV < 400 nm) are used to initiate the photochemical reaction.¹¹ Although these UV-based systems have been well-established in the 3D printing technology, exposure to high energy lights have some shortcomings: (i) UV photons present low penetration depth, and therefore, the accessible layer thicknesses usually remain low (below ~100 μm), resulting in slow 3D printing rate (specifically for large objects); (ii) in the field of 3D bioprinting, the use of UV light also presents risk of cellular photodamage resulting in chromosomal and genetic instability in cells;^{12,13} and (iii) prolonged exposure to high energy UV light might result in side reactions with degradation of reactant and products. Therefore, the development of 3D photopolymerization systems that can be activated under longer irradiation wavelengths has been one of the active research areas in 3D photopolymerization technologies with the aim of: (i) obtaining mild and safe operational condition, (ii) reaching higher penetration depth (layer thickness) resulting in enhancement in the photopolymerization rate, and (iii) providing systems that are benign to living cells for 3D bioprinting applications (i.e., tissue engineering).¹⁴ Moreover, near-infrared (NIR)-induced photopolymerization has emerged as a new strategy, which enables drawing of 3D

Received: November 25, 2018

Accepted: February 20, 2019

Published: February 20, 2019

structures directly in the volume of photocurable materials.^{15–17}

The chemistry of conventional free radical polymerization typically used in the 3D photopolymerization is not “living”; this means the polymer chain is terminated, and consequently, the printed materials cannot be reinitiated to introduce new monomer/functionalities/properties in a living manner. Recently, a “living” system via photoredox catalyzed reversible addition–fragmentation chain transfer (RAFT) photopolymerization has been demonstrated that can be implemented in the 3D printing application. This technique will open a new door for the development of 3D materials with living features.¹⁸

With regards to the recent upsurge of investigations on the photopolymerization-based 3D printing, a comprehensive review from polymer chemistry point of view is critically required. An overview of recent evolutions in the field of photopolymerization-based 3D printing and highlights of novel 3D printable photopolymers is provided herein. 3D photopolymerization systems via radical or cationic systems are discussed. Challenges that limit further development of commonly used photopolymers together with prospective solutions are also elaborated in detail. Research activities and future trends of the 3D photopolymerization are discussed. This review also spotlights recent progress on the controlled living radical photopolymerization techniques suitable for 3D printing. The main themes of this review are represented in Figure 1.

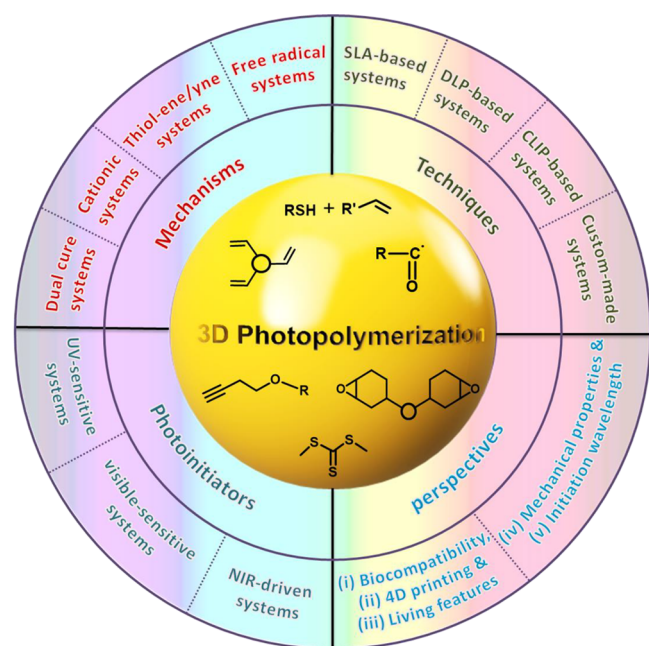


Figure 1. Schematic illustration of the main topics covered in this review.

2. 3D PRINTING TECHNIQUES VIA PHOTOPOLYMERIZATION

Before the discussion on the photochemical mechanisms (Section 3) and photoinitiators used in the 3D-based photopolymerization systems (Section 4), we briefly discuss the main techniques used in 3D printing via photopolymerization. The strategy is based on the light irradiation through a reservoir (vat) filled with photocurable materials, resulting in

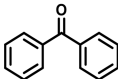
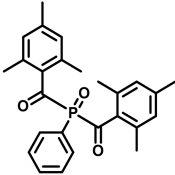
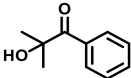
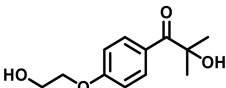
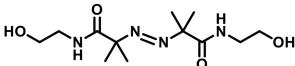
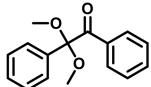
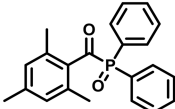
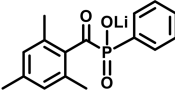
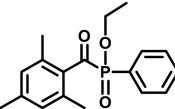
photopolymerization of the liquid monomers/oligomers at a predetermined location, straight on the building platform. This strategy is translated into two streams: SLA and DLP.⁹ For more details about the design architecture and structure orientation of these apparatuses, refer to other reviews.^{19,20} Continuous liquid interface production (CLIP) (Carbon 3D Inc.) has been recently developed as a new resin-bath technique which offers 3D printing speeds up to 100 times faster compared to the DLP and SLA techniques.²¹

Stereolithography. Chuck Hull introduced the first example of SLA 3D printing in 1986.²² SLA is a method and apparatus that uses movable photon source to activate photopolymerization of the photocurable resin and successively print solid layers one on top of the other.²² The first photocurable materials (those used for SLA application) consisted of a urethane dimethacrylate (UDMA) with a small fraction of acrylic acid, benzophenone as photoinitiator, and methyl ethyl hydroquinone/triallyl phosphate (to inhibit premature polymerization).²³ Thus far, various photocurable materials have been developed and exploited in a SLA 3D printing process, which can be used in different applications.²⁴ Using SLA, high-quality objects at a fine resolution as low as 10 μm can be also obtained.²⁵ For example, an SLA-based 3D printer was used to construct high resolution and complex architecture such as a human ear that can be used for tissue engineering.²⁶ SLA technique can be also used to fabricate 3D objects with organic–inorganic hybrid structures such as ferromagnetically responsive formulation.²⁷

Digital Light Processing. DLP method and apparatus has been recently developed, which offers reduced printing times while maintaining high fabrication accuracy.²⁸ The DLP technology features the use of light source illuminating each layer all-at-once as opposed to SLA with point-by-point exposure.²⁹ In a DLP system, photon source illuminates from the bottom of the resin bath, and the building platform is dipped into the resin from above; consequently, the 3D fabrication is feasible with the consumption of low volumes of resins.³⁰ The layer being cured is not in direct contact with air (placed on the bottom of the vat) and therefore is less susceptible to oxygen inhibition.⁵ DLP-based printing has been utilized in a variety of contexts such as fabrication of luminescent 3D structures,³¹ highly stretchable photopolymers,³² engineered nerve guidance conduits,³³ reprocessable thermosets,³⁴ electrically conductive constructs,^{35,36} organic–inorganic hybrid networks,³⁷ and other complex objects.^{38,39} Using DLP-based printers (at 465 nm), patient customized medical devices with an accuracy of $40 \times 40 \mu\text{m}$ can be fabricated, which is desirable for bone scaffolds or medical devices with smooth surfaces.⁴⁰ DLP printers are also compatible for 3D printing of aqueous formulations.³⁸ For instance, a DLP printer was employed for 3D fabrication of poly(ethylene glycol) diacrylate (PEGDA)-based hydrogels under 460 nm LED irradiation (64.2 mW cm^{-2}).³⁸

Continuous Liquid Interface Production. In 2015, DeSimone and coworkers reported a new generation of 3D printing method and apparatus, known as CLIP, that enables “continuous” fabrication of layerless and monolithic polymeric objects.²¹ In a CLIP process, an oxygen-permeable window is used to create an oxygen-containing interfacial layer where free radical photopolymerization is inhibited. Oxygen can inhibit the free radical polymerization by (i) quenching the excited-state photoinitiator or (ii) forming a peroxide upon interaction with a free radical of a propagating chain.⁴¹ Consequently, a

Table 1. Chemical Structures of Common UV Light Photoinitiators Used in 3D Photopolymerization Systems

Name	Chemical Structure	Light absorption (λ_{\max})	Ref.
Benzophenone		253 nm	124
Phenyl bis (2,4,6-trimethylbenzoyl) phosphine oxide (BAPO, Irgacure 819)		295 nm, 370 nm	14,20,36,50,115
2-hydroxy-2-methyl-1-phenylpropan-1-one (Irgacure 1173)		245 nm, 280 nm, 331 nm	36
2-Hydroxy-4'-(2-hydroxyethoxy)-2-methylpropiophenone (Irgacure 2959)		274 nm	9,28,50,116,125–127
2,2'-azobis[2-methyl-n-(2-hydroxyethyl) propionamide] (VA-086)		375 nm	118–121
2,2-dimethoxy-2-phenylacetophenone (Irgacure 651 or DMPA)		252 nm, 340 nm	50,128,129
Diphenyl(2,4,6-trimethylbenzoyl)phosphine oxide (Darocure TPO; Lucirin TPO)		295 nm, 368 nm, 380 nm, 393 nm	20,114,122
lithium phenyl(2,4,6-trimethylbenzoyl)phosphinate (LAP)		375 nm	25,27,121,130–133
Ethyl (2,4,6-trimethylbenzoyl) phenylphosphinate (Lucirin TPO-L)		275 nm, 379 nm	39,134

thin uncured liquid layer remains between the window and the building platform. This oxygen-inhibited dead zone facilitates fast printing speeds and layerless part construction in a continuous manner. Typically, an amorphous fluoropolymer window (such as Teflon AF 2400) with high oxygen permeability, UV transparency, and chemical inertness is used in the oxygen-permeable window.²¹ Using CLIP technique, printed objects can be pulled out of the resin bath at rates of hundreds of millimeters per hour with the production speed in minutes featuring resolution below 100 μm .^{21,42,43}

3. PHOTOPOLYMERIZATION MECHANISMS USED IN THE 3D PRINTING SYSTEMS

3.1. Radical System. **3.1.1. (Meth)acrylate-Based Photocurable Systems.** (Meth)acrylate monomers/oligomers are frequently used for 3D photopolymerization processes which proceed via a radical system. Radical systems include three main steps of radical generation, initiation, and propagation. Radical generation (in photopolymerization) occurs under

light irradiation, in which a photoinitiator or photoinitiator system is responsible to convert photolytic energy into the reactive species to initiate the photopolymerization. Most of the commercially available photoinitiators undergo the Norrish type I α -cleavage reaction and generate radical fragments under light irradiation.^{5,44,45} Depending on the chemical structures of the photoinitiators, the incident light required to induce the cleavage differs in wavelength and intensity. Benzil ketals such as 2-hydroxy-2-methyl-1-phenylpropan-1-one (Irgacure 1173) and 2,2-dimethoxy-2-phenylacetophenone (DMPA; Irgacure 651) with relatively low energy $n \rightarrow \pi^*$ transitions absorb light in the UV range, which are suitable for SLA-based process. Phosphine oxide containing photoinitiators (refer to Table 1) present lower energy level of the π^* state, therefore shifting the peak of the $n \rightarrow \pi^*$ transition toward higher wavelengths, which is preferable for the DLP-based systems.⁵ Two-component photoinitiating systems (known as type II) consist of an uncleavable sensitizer and a coinitiator, which typically form excited triplet states under light exposure.⁴⁶ Most commonly used uncleavable photoinitiators are cam-

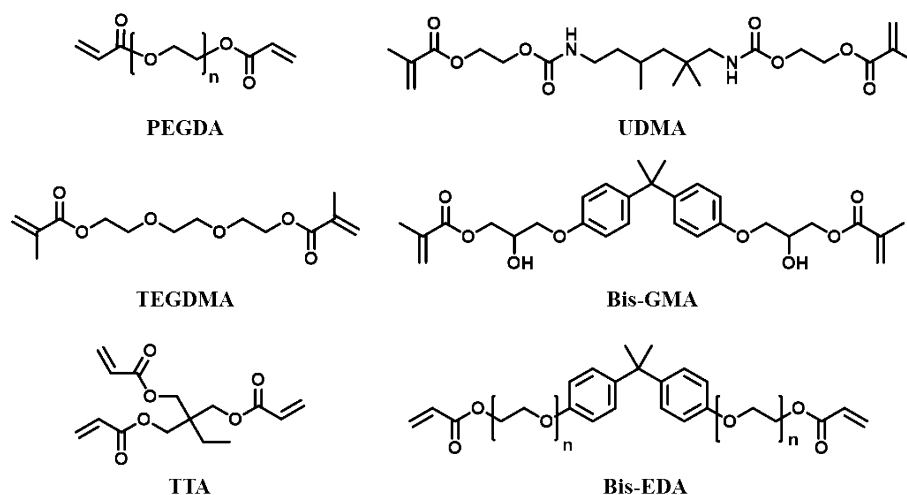


Figure 2. Examples of meth(acrylate) monomer/oligomer typically used in 3D photopolymerization.

phorquinones (CQ), benzophenones and thioxanthenes which are able to undergo hydrogen-abstraction or electron-transfer reactions in the presence of coinitiators (such as tertiary amines).⁴⁴ Combination of the radical photoinitiators can be also used in the photocurable resins. The structures of common photoinitiators are presented in Table 1. The readers who are interested in the structure of the photoinitiators and the mechanism by which a reactive species is formed can refer to other reviews that specifically focused on these aspects.^{5,44,45}

(Meth)acrylate-based resins are compatible with different types of commercially available 3D printers as well as custom-made 3D printers.⁴⁷ These resins have been used in different contexts such as 3D printing of shape memory polymers,⁶ siloxane-based hybrid polymer network,⁴⁸ highly stretchable photopolymers,³² and functional materials for bioapplications.^{49,50} Most common (meth)acrylate monomer/oligomers used in 3D printing are PEGDA,^{26,37,51} UDMA,^{52,53} triethylene glycol dimethacrylate (TEGDMA),^{54–57} bisphenol A-glycidyl methacrylate (Bis-GMA),^{54–57} trimethylolpropane triacrylate (TTA),^{21,43,52} and bisphenol A ethoxylate diacrylate (Bis-EDA)²⁷ (Figure 2).

Although the use of (meth)acrylate-based resins has proved effective in 3D photopolymerization, they have certain limitations. These resins tend to undergo shrinkage during the polymerization. Pure (meth)acrylate resins tend to gel at low conversions depending on the functionality of the monomer used.^{58,59} This phenomenon would normally result in a very limited flow of the remaining uncured resin. Further photopolymerization above this conversion would lead to an increase in shrinkage stress with each newly formed bond. Depending on the molecular structure of the monomer/oligomer, the amount of shrinkage varies. Cycloaliphatic and aromatic acrylates show less shrinkage as compared to the common monomers such as TEGDMA.⁶⁰ Shrinkage and associated stress might result in curling and deformation during the layer-by-layer 3D fabrication.⁶¹ A few strategies have been employed to reduce the shrinkage issues. For instance, the use of high molecular weight oligomeric acrylates (with less reactive group concentration) can reduce the shrinkage percentage; however, heating is required (during the 3D process) to reduce the high viscosity of these resins.⁶² Another approach to lower the amount of shrinkage during the photopolymerization is the use of a radical step growth

mechanism as an alternative to the chain growth polymerization (elaborated in Section 3.1.2).

Most of the (meth)acrylate-based photocurable resins contain multifunctional monomers (i.e., diacrylates and triacrylates) which experience autoacceleration in the early phase of the chain growth (free radical) polymerization due to the fact that termination reactions are mobility restricted.⁶³ The high kinetic chain length would result in the formation of networks with low uniformity and high brittleness, which is less efficient in dissipating stress, and therefore, cracks might propagate more readily.⁵⁹ Regulation of the final polymer architecture can be obtained using chain transfer agents (i.e., addition–fragmentation chain transfer (AFCT)), which have been extensively used for linear polymers.⁶⁴ The use of chain transfer agents in regulating photocurable resins has been also investigated, which showed the ability to tune the cross-linking density, average kinetic chain length, and distribution of cross-links alongside the backbone, suggesting a homogeneous polymer architecture with lower brittleness (elaborated in Section 3.1.3).⁶⁵

Another limitation of (meth)acrylate free radical polymerization is the oxygen inhibition.⁶⁶ One possible solution to tackle this issue is the use of additives (such as tertiary amines or triphenylphosphine⁶⁷) to lessen the oxygen inhibition in the open vat 3D systems. However, tertiary amines are not suitable for resins containing both (meth)acrylate/epoxy materials (this kind of resin is commonly used commercially⁶⁸) due to the inhibition effect of amines on the cationic polymerization.⁶⁹ Moreover, the use of tertiary amines might result in discoloration of the cured material.⁷⁰ Photopolymerization systems based on the “thiol–ene” chemistry can also reduce the oxygen inhibition (refer to Section 3.1.2).⁷¹ This strategy is useful where the resin is in direct contact with air; however, it is not practical for CLIP where oxygen inhibition is essential to avoid adhesion of the curing platform to the bottom of the resin vat.²¹

3.1.2. Thiol–Ene and Thiol–Yne Systems. Reactions of thiols with reactive carbon–carbon double bonds, or “enes”, are well-established.⁷² These reactions can proceed via a radical step-growth polymerization or Michael-addition reactions.^{59,73} Thiol–ene-based photocurable resins have some advantages over (meth)acrylate-based formulations. First, thiols act as potent hydrogen donors to a formed peroxide radical and generate a reactive thiyl radical, therefore

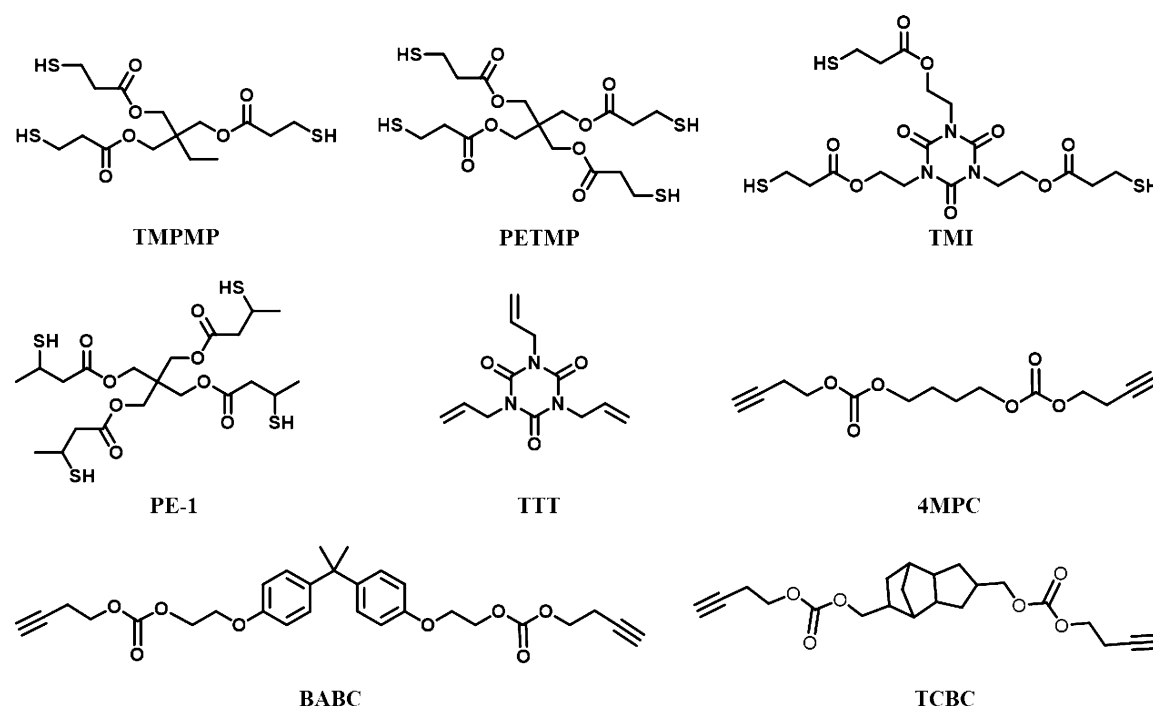


Figure 3. Examples of thiol and ene/yne monomers typically used in 3D photopolymerization.

alleviating the oxygen inhibition.⁷⁴ Second, thiol–ene-based resins show lower shrinkage stress as compared to that of acrylate-based resins. This is mainly due to the occurrence of gel point at relatively high conversion (>30%), resulting from the step growth mechanism of the thiol–ene systems.⁷⁵ Third, thiol–ene systems show higher biocompatibility as compared to the (meth)acrylate-based networks.⁴⁰ These advantages have made the thiol–ene chemistry as an attractive approach for the fabrication of different 3D structures such as biocompatible and biodegradable hydrogel constructs,^{76,77} optical waveguides,⁷⁸ and woodpile photonic crystals.⁷⁹ Common thiol monomers suitable for the 3D printing are trimethylolpropane tris(3-mercaptopropionate) (TMPMP),^{80,81} pentaerythritol tetra(3-mercaptopropionate) (PETMP),⁴⁰ tris[2-(3-mercaptopropionyloxy) ethyl] isocyanurate (TMI),⁸² and pentaerythritol tetrakis(3-mercaptopropionate) (PE-1)⁸³ (Figure 3).

Besides the aforementioned advantages that the thiol–ene-based systems offer, there are few issues that hinder their further development in the 3D applications. Among these issues are poor shelf life (due to an oxidative disulfide bond formation) and bad odor. Moreover, these systems form homogeneous networks (via step growth kinetics) with flexible thioether linkages which might result in the formation of soft materials with low modulus.^{80,84} However, low modulus of these systems can be improved by addition of a meth(acrylate) monomer into the binary thiol–ene systems and form a ternary system.⁷³ Another strategy to improve the mechanical properties of the thiol–ene systems is by polymerizing norbornene end-capped oligourethanes with TMPMP.⁸⁵ This can create a strong hydrogen bonding between urethane chains and therefore increase the rigidity of the formed network.⁸⁵ Poor shelf life stability of the primary thiols can be improved by the use of stabilizers^{86,87} or developing new monomer systems. Recently, Li and coworkers synthesized highly stable secondary thiol–ene photocurable systems (e.g., PE-1 and

triallyl-1,3,5-triazine-2,4,6 (1*H*,3*H*,5*H*)-trione (TTT) (Figure 3), which showed better thermal storage stability (>7 days) at 60 °C than the primary thiol–ene system (thiol–ene formulation of: PETMP/TTT) (<3 days).⁸³ Lower shrinkage (~7.6%) also observed as compared to the traditional acrylate system (~13.9%). The developed secondary thiol–ene systems were used in a DLP 3D printing (420 nm) to construct objects with a Z resolution of 50 μm.⁸³

Alkyl thiols also undergo addition reactions with carbon–carbon triple bonds, enabling thiol–yne chemistry. The reaction intermediate is a vinyl sulfide with the ability to undergo a second addition with excess thiol. This phenomenon generates more cross-linked network, resulting in a higher glass transition and higher modulus as compared to those of the thiol–ene-derived products.^{88,89} For instance, Griesser and coworkers synthesized alkyne carbonate derivatives (e.g., 1,4-butanediol dipent-4-yn-2-yl carbonate (4MPC) or 2,2-bis[4-(2-hydroxy)ethoxyphenyl]propane dibut-3-yn-1-yl carbonate (BABC)) (Figure 3) as biocompatible and biodegradable building blocks participated in a thiol–yne photopolymerization reaction, which was initiated under blue light irradiation (465 nm) in a DLP printer.⁴⁰ Benefiting from the thiol–yne photopolymerization, 3D printed products based on the tricyclo[5.2.1.0^{2,6}]decane-4,8-dimethanol dibut-3-yn-1-yl carbonate (TCBC) (Figure 3) showed high toughness similar to polylactic acid (thermoplastic biopolymer which is commonly used as a polymeric implant material). This system also showed cytotoxicity lower than that of their corresponding meth(acrylates).⁴⁰

3.1.3. Addition–Fragmentation Chain Transfer (AFCT). Knowing that (meth)acrylate-based photocurable systems produce brittle materials (due to their inhomogeneous and highly cross-linked network structure), efforts have been devoted to improve the homogeneity and therefore the toughness of the 3D materials to meet the requirements of different applications. AFCT reagents (such as oxybis(ethane-

2,1-diyl))bis(oxy))bis(ethane-2,1-diyl)bis(2-(tosylmethyl)acrylate) and ethyl 2-(tosylmethyl)acrylate (ester activated β -allyl sulfone, EAS)) can be incorporated into a (meth)acrylate⁶⁵ or thiol-ene systems^{90,91} to regulate the radical network formation (via chain transfer reaction). Use of AFCT results in the formation of homogeneous networks and hence provides high toughness networks.^{92,93} The implementation of chain transfer via the AFCT mechanism can also reduce the shrinkage stress observed in the free radical photopolymerization systems.⁶⁵ Incorporation of AFCT agents into the (meth)acrylate formulations proceeds via a radical step growth-like mechanism without the problems of low storage stability and strong odor (present in the thiol-ene chemistry).⁸⁶ However, due to the inherent mechanism of AFCT-based polymerization,⁶⁵ the overall curing time for AFCT containing resins proceed with retardation, which is not desirable for 3D-based applications with the need of high rate photopolymerization. To solve the issue of retardation, Liska and coworkers synthesized an AFCT reagent that could proceed with an alternative radical mechanism with high reaction rate. By replacement of the methylene group of EAS with an oxygen atom, giving a vinyl sulfone ester (such as ethyl 2-(tosyloxy)acrylate (ethyl ester activated vinyl sulfonate or EVS)), a carbonyl bond would be generated after the AFCT reaction due to the oxygen atom making the reaction nonreversible and consequently driving the reaction equilibrium toward fragmentation.⁶⁵ Fabricated EVS was used to initiate the radical photopolymerization of commercial dimethacrylates (UDMA and 1,10-decanediol dimethacrylate) with Ivocerin photoinitiator in a DLP 3D-based experiment. 3D photopolymerization proceeded at a higher rate (as compared to the EAS-based resin), which produced 3D objects with tough and homogeneous networks.⁶⁵

3.2. Cationic Systems. Cationic photopolymerization was first established using cationic photoinitiators of aryl iodonium salts or sulfonium photoinitiators^{94–97} which can decompose under UV light irradiation to produce reactive species. Besides their use in coatings, these systems have also been used in 3D applications,^{98,99} with commercially available epoxy monomers such as 3,4 epoxycyclohexane)methyl 3,4 epoxycyclohexylcarboxylate (EPOX)^{57,100–102} and bisphenol A diglycidyl ether (DGEBA)¹⁰³ (Figure 4). Depending on the molecular

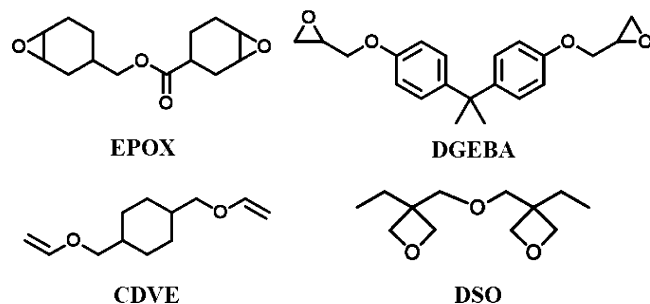


Figure 4. Examples of monomers used in cationic 3D photopolymerization.

structure of the monomers, their reactivity differs; for instance, monomers with cycloaliphatic epoxides have high double ring strain and undergo fast polymerization.⁵⁹ Besides, cationic polymerizable vinyl ether monomers such as 1,4-cyclohexane dimethanol divinyl ether (CDVE) have been commonly used in the SLA-based systems.¹⁰⁴ For instance, CDVE can be used

in combinations with epoxides to enable fast polymerization (Figure 4).¹⁰⁴ Moreover, disubstituted oxetane (DSO; Figure 4) monomers can be used in cationic photopolymerization which offer high reactivity (compared to the epoxides) with comparable low shrinkage rate and improved water resistance.^{105,106} The interest in using epoxide monomers originates from their low volumetric shrinkage ($\sim 3\%$) that occurs during ring opening photopolymerization.¹⁰⁰ For instance, to limit/avoid the shrinkage effect that is usually observed in the 3D printed objects via free radical polymerization, Al Mousawi et al. reported the use of azahelicenes in combination with bis(4-*tert*-butylphenyl)-iodonium hexafluorophosphate (Iod) as visible light photoinitiators to initiate the cationic polymerization of EPOX to fabricate 3D printed objects.¹⁰⁰

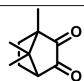
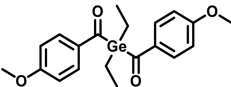
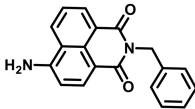
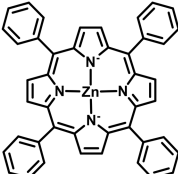
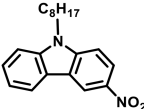
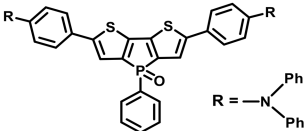
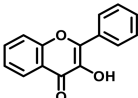
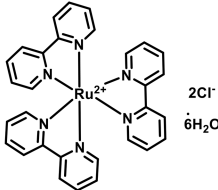
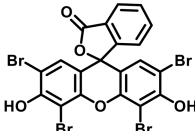
In theory, the cationic curing process proceeds in a chain growth mechanism with high number of cross-linking points along the polymer backbone, resulting in increased brittleness. To lessen the cross-linking density, chain transfer agents (such as polyester and polyether diols) can be used at low concentrations (5–20 wt %).⁹⁹ The photocurable systems containing more than one type of monomer with different reactivity (but similar type of photopolymerization mechanism which form copolymer) have been extensively used to regulate the polymerization rate and tune the properties of the final 3D products, i.e. lowering the curl factors.¹⁰⁷ Besides these systems, the use of photocurable systems containing more than one type of monomer with different polymerization mechanism has been also investigated.¹⁰⁸ These dual cure formulations (for instance combination of cationic monomer of bicycloaliphatic diepoxide and radical-type monomer of bisphenol A diacrylate derivative⁶⁸) can form interpenetrating networks to adjust the photopolymerization rate and cross-linking density and therefore control the final properties suitable for different applications.¹⁰⁹ Moreover, to avoid the incompatibility of the two different types of monomers, hybrid monomer 3,4-epoxy-cyclohexylmethyl methacrylate (containing both epoxide and methacrylate groups), which can undergo both cationic and free-radical photopolymerization, can be used.¹¹⁰ It should be noted that cationic initiators can be used in combination with the type I radical initiators, in which radical intermediates generated from radical initiator may react with iodonium or sulfonium cationic reagents to generate radical cations.⁵

4. PHOTOINITIATORS USED IN 3D PRINTING

As elaborated above, photopolymerization reactions can be either radical or cationic. Initiation occurs under light irradiation, in which a photoinitiator or photoinitiator system is responsible to convert photolytic energy into the reactive species.¹¹¹ The light source can be in a form of xenon lamps, mercury arc lamps, LEDs, or lasers. The wavelengths of photon source can be within UV (190–400 nm), visible (400–700 nm), or IR range (700–1000 nm).¹¹² In the following sections, we present an overview of the photoinitiating systems mentioned in the literature for 3D applications. For more details about the mechanisms involved in the photoinitiation reactions, refer to other reviews.^{44,45,113,114}

4.1. UV Light-Sensitive Photoinitiator. A number of commercially available UV-light-sensitive photoinitiators have been used in 3D applications (Table 1).^{115,124–135,160,161} The first photocurable materials reported by Hull contained benzophenone (Table 1) as a photoinitiator which was initiated under a 350 W mercury short arc lamp photon

Table 2. Examples of Visible Light Photoinitiators Used in 3D Photopolymerization Systems

Name	Chemical Structure	Light absorption (λ_{\max})	Ref.
Camphorquinone (CQ)		468 nm	14,51,159,160
Bis (4-methoxybenzoyl) diethylgermanium (Ivocerin)		408 nm	39,141
5-amino-2-benzyl-1H-benzo[de]isoquinoline-1,3(2H)-dione (NDP2)		417 nm	14
Zinc tetraphenylporphyrin (ZnTPP)		420 nm	97
3-nitro-9-octyl-9H-carbazole (C2)		375 nm (broad absorption within 350–450 nm)	55
2,6-bis (triphenylamine) dithieno[3,2-b:2',3'-d] phosphole oxide (TPA-DTP)		465 nm	53
3-hydroxyflavone (3HF)		$\lambda_{\max} = 350$ nm (broad absorption within 370–470 nm)	56
Tris (2,2-bipyridyl) dichlororuthenium (II) hexahydrate (Ru)		453 nm	12,76
eosin Y		524 nm	121

source for SLA application.²² This work was extended with a more efficient photon source (He–Cd laser) to cure resins that absorb at 325 nm.²³ Chiapponne and coworkers have used two different photoinitiators, namely bis(2,4,6-trimethylbenzoyl) phenylphosphine oxide (Irgacure 819; BAPO; Table 1) with absorption in the deep blue to near UV and Irgacure 1173 (Table 1) as a UV-sensitive compound, to initiate the photopolymerization of PEGDA in a DLP process.³⁷ Chiapponne and coworkers also reported the use of Irgacure 819 to initiate the photopolymerization of PEGDA in the presence of silver nanoparticle precursors via a DLP system.¹¹⁶ 3D printed structures were thermally treated to induce in situ generation of silver nanoparticles within the polymer matrix and thereby provide electrical conductivity.¹¹⁶

Bashir and coworkers reported the use of a commercially available UV-sensitive photoinitiator, 2-hydroxy-4'-(2-hydroxyethoxy)-2-methylpropiophenone (Irgacure 2959; Table 1) for the photopolymerization of PEGDA hydrogels using an SLA process.¹¹⁷ In their approach, NIH/3T3 cells were homogeneously distributed within the structure of hydrogels which showed improved cell viability, proliferation, and spreading.¹¹⁷ In another study by the same group, a UV-curable polymer solution was prepared consisting of Irgacure 2959 photoinitiator, a mixture of acrylic-PEG-collagen solution and PEGDA. This photopolymer solution was cured under UV laser irradiation (325 nm) for the fabrication of biohybrid cantilevers.¹¹⁸ Besides Irgacure 2959 with high biocompatibility, 2,2'-azobis[2-methyl-*n*-(2-hydroxyethyl) propionamide]

(VA-086; Table 1) photoinitiator has been exploited in biocompatible 3D printing systems, which has low cytotoxicity and higher absorption peak (375 nm).^{119–122} Another water-soluble photoinitiator is Irgacure 651 (DMPA; Table 1) which has been used in different 3D printing systems, for example, in fabrication of biocompatible hydrogel scaffolds with fractal geometries.⁵¹

Another common UV-sensitive photoinitiator is diphenyl (2,4,6-trimethylbenzoyl)phosphine oxide (Darocure TPO; Table 1).^{21,115,123} Recently, Lee and coworkers reported the potential use of Darocure TPO photoinitiator for SLA-based 3D printing.¹²⁴ Although this photoinitiator was originally intended as a UV photoinitiator, its absorption up to 420 nm was sufficient to generate radical under visible light irradiation (>400 nm) and induce the photopolymerization of pentaerythritol tetraacrylate (PETA) and 1,6-hexanediol diacrylate (HDA). Darocure TPO has the advantage of being colorless which offers 3D fabrication of objects with optical transparency. Usually, 3D printed constructs with high mechanical toughness are mostly nontransparent or partially transparent, while 3D objects with high optical transparency are mostly PEG-based with soft mechanical properties, restricting potential bioapplications in tissue engineering. Using Darocure TPO, the printed constructs showed high transparency with high mechanical properties as compared to the typical 3D hydrogel objects prepared using Irgacure 2959. Some of the photopolymerization reactions require more complex photoinitiating systems. For instance, a mixture of compounds was required to initiate the photopolymerization of PEGDA resin combined with cellulose nanocrystals (CNC) in a SLA-based 3D printing (laser at 405 nm).²⁶ The photoinitiating system was modified to absorb light at longer wavelength than UV light, which contains lithium phenyl(2,4,6-trimethylbenzoyl)phosphinate (LAP, Table 1), disodium (3Z)-6-acetamido-4-oxo-3-[[4-(2-sulfonatoxyethylsulfonyl) phenyl] hydrazinylidene] naphthalene-2-sulfonate (RO16), and (2,2,6,6-tetramethyl 1-piperidinyloxy) (TEMPO).²⁶ LAP with water solubility was used to create a balance between photon absorptivity and biocompatibility, while RO16 and TEMPO were added to regulate the photopolymerization reaction. Complex architecture such as a human ear construct has been 3D printed using this system that can be used for tissue engineering.²⁶

4.2. Visible Light-Sensitive Photoinitiators. Polymerization under visible light irradiation has witnessed huge interest in the past few years.^{136–138} Use of visible light can circumvent the limitations aroused from high-energy UV light exposure and reduces the risks of eye damage. As compared to the UV light, visible LEDs are eco-friendly and do not release ozone while have low thermal effect with long lifetimes. Moreover, lights with longer wavelengths are also more benign to living cells and are preferable for biomedical applications and dentistry.^{14,139,140} Due to these benefits, the use of visible light in 3D applications has emerged by taking advantage of visible light-sensitive photoinitiators (Table 2).^{14,38,40,100,101} These visible light photoinitiators were commonly used in research laboratories, and there is plenty of room for their development industrially.

Liska and coworkers have reported the use of a bimolecular photoinitiator system consisting of CQ (Table 2) with visible light absorption and a tertiary amine such as ethyl 4-dimethylaminobenzoate (DMAB) to initiate the photopolymerization under visible light irradiation.¹⁴¹ However,

this system suffers from some limitation such as toxic effect, the tendency for discoloration of the amine-based coinitiator and low reactivity.¹⁴¹ Alternative titanocenes photoinitiators can absorb up to 560 nm; however, discoloration of the cured material using this system (due to the photobleaching effect of the photoinitiators) has limited its application.⁷⁰ Liska, Stampfl, and coworkers reported the use of a 400 nm LED array to initiate three different photoinitiators such as Ivocerin (Table 2), BAPO, and TPO-L to simulate the 3D printing process of Cubiflow resin (a commercial available 3D printing resin based on difunctional methacrylates).¹⁴² Because the absorption of these photoinitiators weakly tails out at ~420 nm, these are not effective under some LED sources with long wavelength.⁷⁰

Recently, Xiao et al. reported the use of naphthalimide derivatives (1,8-naphthalimide derivatives bearing a methacrylate functional group) as light-sensitive photoinitiators.^{108,143} The derivatives with the alkylamino substituent at the 4-position combined with an iodonium salt, *N*-vinylcarbazole (NVK), amines, or 2,4,6-tris(trichloromethyl)-1,3,5-triazine were employed to induce the cationic or radical photopolymerization under visible light sources (such as soft halogen lamp, laser diode at 457 nm, laser diode at 405 nm, or blue LED bulb at 462 nm). The reported combinations showed better performance as compared to the CQ/amine or CQ/iodonium salt photoinitiator systems.^{108,143} Enlightened by these findings, different naphthalimide derivatives were further synthesized and introduced into two- or three-component photoinitiating systems in combination with an iodonium salt (and optionally NVK) or an amine (and optionally chlorotriazine) to generate reactive species (radicals and cations) under visible light irradiation.¹⁴ These photoinitiating systems were effective to initiate the cationic polymerization of epoxides (i.e., EPOX) or the free radical polymerization of acrylates (i.e., TTA) under different photon sources (such as LED at 385, 395, 405, 455, or 470 nm or the polychromatic visible light from the halogen lamp).¹⁴ The naphthalimide derivative with an amino substituent (5-amino-2-benzyl-1*H*-benzo[de]isoquinoline-1,3(2*H*)-dione (NDP2); Table 2) combined with diphenyliodonium hexafluorophosphate and NVK were selected to initiate the free radical photopolymerization of TEGDMA/tricyclodecane dimethanol diacrylate (under air) using a 3D printer with LED projector at 405 nm.¹⁴

While photoinitiators with organic structures are commonly used in industrial light curing applications, organometallic photoinitiators (photoredox catalysts) have been extensively exploited in laboratory experiments.¹⁴⁴ These metal complexes offer promising photochemical properties such as strong visible light absorption, relatively long-lived excited states, and suitable redox potentials.^{136,145} These compounds can react as photoredox catalysts (through either an oxidation or a reduction cycle)^{146–148} to produce active species and thus drive various photopolymerization systems such as photoinduced atom transfer radical polymerization (ATRP), photoinduced RAFT, and other polymerization systems.^{149–154} The use of photoredox catalysts was also explored in the light curing 3D applications. For instance, a photoinitiating system based on copper complexes bearing pyridine-pyrazole ligands (with relatively high absorption within 350–600 nm range) was used as a photoredox catalyst to initiate the free radical polymerization of (meth)acrylates and the cationic polymerization of epoxides under 405 nm LED irradiation.⁵⁵

Al Mousawi et al. reported the potential use of zinc tetraphenylporphyrin (ZnTPP; Table 2)^{138,155} combined with Iod as an efficient photoinitiator system to initiate the free radical polymerization of Bis-GMA and TEGDMA. Combination of ZnTPP with Iod was also used to initiate the cationic polymerization of EPOX using a 3D-based LED projector (405 nm).⁹⁸ Although the use of metal-based photoinitiators has shown promise in activating photochemical reactions, their further development is restricted due to the presence of a metal in their chemical structure, which may result in potential toxicity, low storage stability, and bioaccumulation (in biorelated application).^{156–158} Consequently, the development of metal-free photoinitiators and organic photoredox catalysts that can be used in 3D application has been investigated.^{54,56,98,102}

Enlightened by the use of carbazole derivative as a photoredox catalyst used in ATRP,¹⁵⁹ Lalevée and coworkers developed new carbazole derivatives with different substituents as a metal-free photoredox catalyst, which is active in both oxidative and reductive cycles.⁵⁶ The presence of a secondary amine group $N(C_8H_{17})_2$ as an electron donating group and a nitro group NO_2 as an electron accepting group results in a red-shifted absorption and broadening of the absorption peaks in the visible range (due to the increase in a push–pull effect⁵⁶). These derivatives showed absorption in the 350–500 nm range with high extinction coefficients (i.e., $\sim 7800 M^{-1} cm^{-1}$ at 405 nm for the carbazole derivatives with halogen substituents). A developed carbazole derivative, 3-nitro-9-octyl-9H-carbazole (C2; Table 2) (extinction coefficients $\sim 11\,100 M^{-1} cm^{-1}$ at 375 nm and $\sim 5100 M^{-1} cm^{-1}$ at 405 nm) combined with Iod were used in a 3D printing experiment (LED projector at 405 nm) to initiate the cationic polymerization of EPOX under air.⁵⁶

Despite the successful implementation of these metal-free carbazole derivatives in the 3D printing experiments, accessible penetration depth remained relatively low (about 600 μm for the thickest 3D resolved sample).^{56,102} Lalevée and coworkers reported a new generation of metal-free photoinitiators based on luminescent dithienophosphole derivatives. Due to the high degree of π -conjugation, these photoinitiators showed long wavelength absorption in the near-UV or visible ranges (depending on the substituents) with photoluminescent properties. Remarkably, 2,6-bis(triphenylamine)dithieno[3,2-b:2',3'-d] phosphole oxide (TPA-DTP; Table 2) showed a broad absorption between 350 and 600 nm, with a very high extinction coefficient ($\sim 30\,000 M^{-1} cm^{-1}$) at 465 nm. Combination of TPA-DTP with Iod was effective to initiate the free radical polymerization of methacrylates (Bis-GMA/TEGDMA 70%/30% w/w) under air in a laser-based 3D experiment (405 nm). Notably, using this photoinitiating system a well-resolved thick sample (up to ~ 2 mm) was 3D printed in a short printing time (< 1 min for a 2 cm length logo).⁵⁴ In another approach, Al Mousawi et al. reported the use of naturally derived 3-hydroxyflavone (3HF; Table 2) as a visible light initiator.⁵⁷ 3HF compound offers a few unique properties such as (i) long wavelength absorption in the visible range, (ii) biocompatibility, and (iii) low toxicity, which makes it an excellent candidate for safe 3D printing applications. 3HF combined with an amino acid (*N*-phenylglycine, NPG) was used to initiate the free radical polymerization of Bis-GMA/TEGDMA under air with 1.4 mm-thick samples (LED projector at 405 or 477 nm). The 3HF/NPG system offered fast photopolymerization rate, resulting in methacrylate

conversion of $\sim 71\%$ after 100 s of irradiation with LED at 405 nm.⁵⁷ Besides the aforementioned systems, a number of photoinitiating systems with the ability to absorb in the visible range and initiate 3D photopolymerization (such as Tris(2,2-bipyridyl) dichlororuthenium(II) hexahydrate (Ru)^{12,77} and eosin Y¹²²) have been investigated (Table 2). However, there is still plenty of scope for further innovative studies in the development of 3D photopolymerization under light with higher wavelengths (see Section 6.5).

5. NIR-DRIVEN 3D PHOTOPOLYMERIZATION SYSTEMS

NIR light offers advantages over UV and visible light with less photodamage, lower scattering, and higher penetration depth.¹⁶ One possible way to use NIR light in a 3D process is the use of two-photon initiators.¹⁶² The idea of two photon absorption (TPA) was first predicted by Maria Göppert-Mayer,¹⁶³ which was further developed after the availability of solid-state femtosecond pulsed lasers required to activate the nonlinear TPA process. Taking advantage of the TPA process, two-photon polymerization (2PP) has been extensively explored.^{164,165} This technique has also been used in 3D printing application,^{52,166} and 3D printer manufacturers (such as Nanoscribe) use 2PP 3D printing technology in their systems for microfabrication. We refer readers to few comprehensive reviews for further information.^{165–167}

Although 2PP process has the advantage of using NIR light, its application is limited due to (i) the small TPA cross sections of common chromophores and their high fluorescence quantum yields (Φ_F),¹⁶⁸ resulting in a long curing process, and (ii) the necessity of using expensive pulsed NIR lasers at high intensities. One possible solution to overcome these issues is the use of lanthanide-doped upconversion nanoparticles (UCNPs).¹⁴⁰ UCNPs have the ability to “sequentially” absorb two or more low energy NIR photons and emit high-energy light in the UV, visible, and shorter wavelengths of NIR (800 nm).^{138,169} As opposed to the two-photon process, UCNPs can be excited with a relatively moderate intensity continuous-wave lasers (several orders of magnitude lower than that for simultaneous TPA).¹⁴⁰ The excitation light required to stimulate UCNPs (usually centered at 975 nm for ytterbium-sensitized UCNPs), corresponds to the low-loss optical window of frequently used monomers and polymers, suggesting minimal absorption and scattering loss by the polymeric materials.¹⁷⁰ Due to these properties, UCNPs have been used to initiate the photopolymerization of various monomers^{171–176} and photocurable materials¹⁷⁷ and very recently used to construct 3D objects.^{178–179}

For example, Méndez-Ramos and coworkers demonstrated the use of UCNPs as a localized UV light source for 3D fabrication of PEGDA-based resin. Under 980 nm laser exposure, upconverted UV/blue emissions (290–360 nm) from thulium (Tm)-doped UCNPs, which overlap with the absorption of Irgacure-819 photoinitiator, was used to initiate the photopolymerization of PEGDA. A qualitative demonstration of UCNP-assisted NIR-activated 3D fabrication was also proved.¹⁷⁸ Khaydukov, Guller, and coworkers also reported the use of NIR light and UCNPs to initiate a 3D printing process.¹⁷ Upon 975 nm irradiation, upconverted emissions (288, 345, and 360 nm) initiated the Darocure TPO photoinitiators present in a commercially available photocurable resin (E-shell 300, EnvisionTEC) and consequently activated the photopolymerization process. Using this

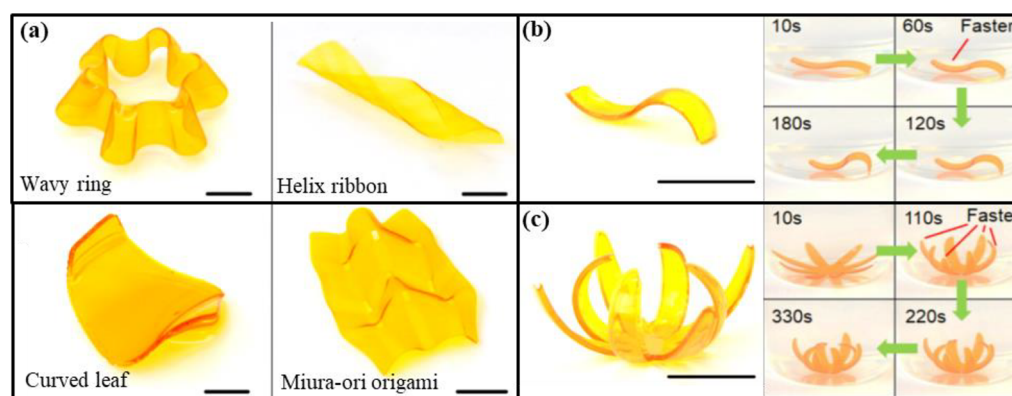


Figure 5. (a) 3D hydrophilic/hydrophobic composite shape-shifting structures (scale bar: 10 mm). (b) A strip that deformed to “S” shape after swelling in water. A sequential water-responsive “S” strip. (c) A sequential water-responsive flower (scale bar: 10 mm). Reproduced with permission from ref 199. Copyright 2018, American Chemical Society.

approach, macro- and microstructures were printed using layer-by-layer drawing directly in the resin volume.¹⁷ In a recent patent, Tumbleston and coworkers also exploited UCNPs (i.e., NaYF₄:Yb/Tm) as a localized light source to initiate 3D photopolymerization of various types of photocurable resins (such as PEGDA).¹⁷⁹

6. EVOLUTION AND FUTURE DIRECTION OF 3D PRINTING USING PHOTOPOLYMERIZATION

As elaborated above, various photocurable formulations have been used in a 3D printing process, offering different chemical and mechanical properties. Although developed systems show great promises in 3D applications, they cannot fulfill all the desired requirements of the final products. Therefore, to further extend and expand the scope of 3D printing applications, more innovative studies are required to tailor the final properties of the 3D printed materials. The areas and opportunities that require further exploration are (i) improving the biocompatibility of the 3D printed materials, (ii) further development of 4D printing, (iii) design of the 3D printable materials with living features using controlled living radical polymerization techniques, (iv) tuning the physicochemical and mechanical properties of the 3D printed materials, and (v) shifting the initiation wavelength required to activate the 3D photopolymerization toward longer wavelengths.

6.1. Photocurable Formulations with Enhanced Biocompatibility. 3D bioprinting is a term referring to techniques used for 3D fabrication of biocompatible materials, functional tissues, and organs with precise control over the deposition of cells.^{13,180,181} The development of 3D bioprinting has attracted attention in applications such as tissue engineering and regenerative medicine.^{180–182} However, available photocurable resins are mostly restricted for bioapplications due to their low biocompatibility, transparency, elasticity, etc. Commonly used (meth)acrylate resins show high irritancy levels or even cytotoxicity in the uncured state.^{40,77,183} Leakage/leaching of the unreacted monomer/oligomer (as a result of low conversions of these resins) can cause health risks when they are in direct contact with the human body. Possible hydrolytic degradation of the (meth)acrylate-based complex leads to the formation of (meth)acrylic acid which can decrease the local pH and adversely affect the physiological properties.¹⁸⁴ Biodegradation of polymer materials (such as implanted material) is another important factor limiting the regenerative medicine and tissue engineering.⁷⁶

Moreover, only limited commercially available photoinitiators show adequate water solubility and biocompatibility.³⁸ Therefore, specialized biomaterials (otherwise known as bioinks in the 3D field) with specific rheological, biological, mechanical, and chemical properties alongside with high biocompatibility must be developed.

Among various biocompatible polymers that are approved by United States Food and Drug Administration (FDA) and can be used for clinical applications (e.g., polycaprolactone, poly(lactic acid) and poly(glycolic acid)), PEG-based materials offer hydrophilicity, biocompatibility, and ability to be chemically functionalized.^{185,186} The use of PEG-based 3D materials has been also explored using SLA and DLP processes.^{26,50,118,187,188} For instance, using SLA-based 3D printing, Basit and coworkers fabricated PEGDA-based tablets (encapsulating 4-aminosalicylic acid and paracetamol as model drugs) with a controllable drug release profile.¹⁸⁹ Further, gelatin-based systems show high water solubility and are also known to support cell adhesion and proliferation.¹⁹⁰ These features make them a suitable candidate for 3D bioprinting. For instance, methacrylated gelatin (GelMA) was employed to fabricate biocompatible 3D hexagonal liver lobule-like tissue consisting of hepatocytes and supporting cells via a DLP-based process.¹⁹⁰ The diversity and applicability of the available biocompatible and biodegradable formulations are limited, and further investigation into the biocompatible 3D printable systems is greatly demanded.

6.2. 4D Printing. 4D printing with the fourth dimension being time has been developed in the past few years.^{191,192} 4D printing offers a 3D printed object to evolve its shape, property, and functionality with time in response to an external stimulus such as water, temperature, pH, light, etc.^{193–198} For instance, Fang and coworkers synthesized solvent-responsive shape-shifting 3D structure which can be patterned using a DLP projector.¹⁹⁹ In their approach, hydrophilic PEGDA and hydrophobic poly(propylene glycol) dimethacrylate were photopolymerized to form a bilayer hydrophilic/hydrophobic composite. This composite showed a strain mismatch during swelling that can induce a controlled shape shifting (Figure 5).¹⁹⁹ Using a SLA printer, Magdassi and coworkers reported the 3D fabrication of shape memory objects using methacrylated polycaprolactone, which can be used in flexible and responsive electrical circuits.⁶ In microfluidic field, valves that are capable of controlling flow in response to changes in the flowing solution are of practical importance. Cohn and Dutta

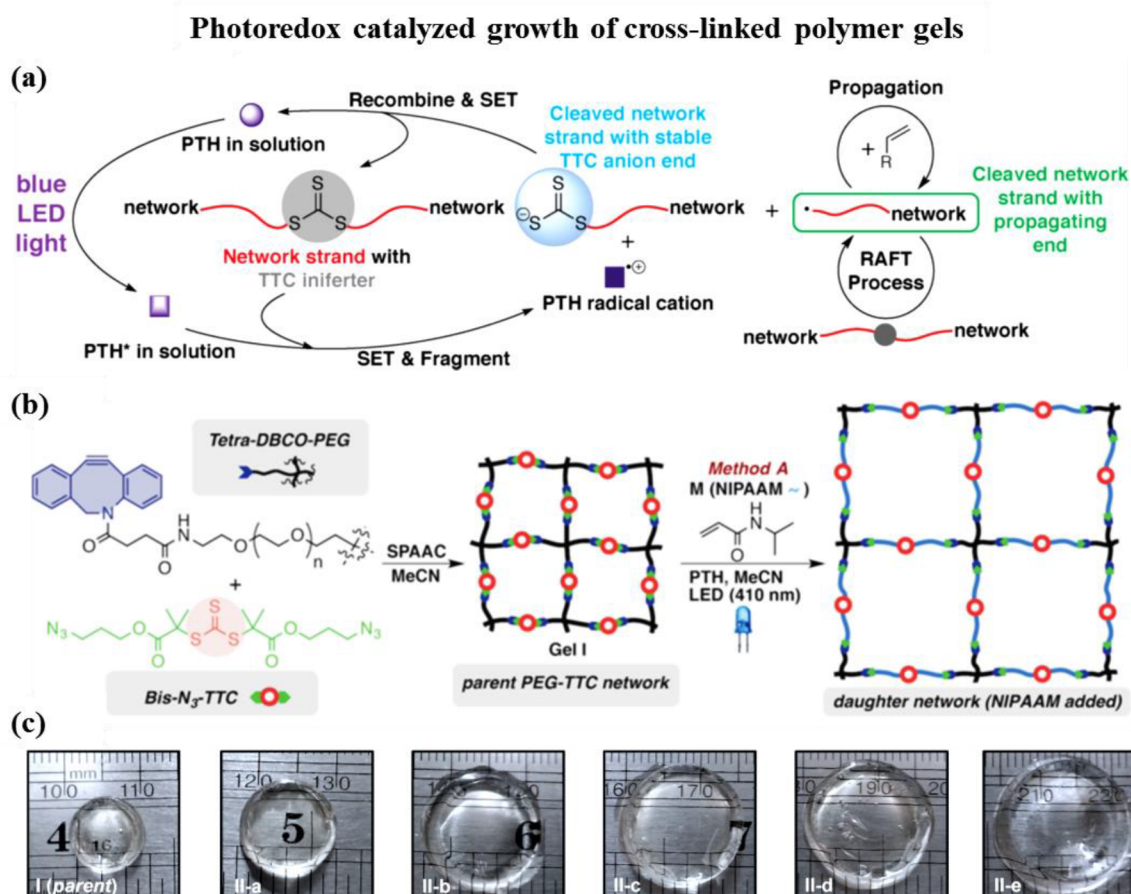


Figure 6. Photoredox catalyzed growth (PRCG) of cross-linked polymer gels. (a and b) Proposed mechanism of PRCG polymerization using PTH and a network comprised of strands bearing TTC iniferters. (c) Optical images of parent gel I and daughter gels swollen in pure water at 20 °C. Reproduced with permission from ref 18. Copyright 2017, American Chemical Society.

fabricated a 3D printed macroscopic valve (using a SLA printer) composed of dually responsive hydrogels with the ability to respond to the fluctuations in temperature and pH. This valve consisted of the reverse thermoresponsive methacrylated poly(ethylene oxide)-poly(propylene oxide)-poly(ethylene oxide) which was copolymerized with acrylic acid as a pH-sensitive monomer. Due to the “on demand” responsiveness and ability to change in size and geometry, these hydrogels can be used in medical device field.¹⁹⁷

Besides the aforementioned features, 4D bioprinting is a useful tool for biomedical applications due to their ability for postmaturation of printed cell populations within the printed scaffolds.²⁰⁰ With the involvement of time, living cellular constructs can continue to evolve after being printed, facilitating the fabrication of tissue constructs with properties that are similar to the native tissues.²⁰⁰ However, current photocurable materials and printing technologies suitable for 4D printing are limited. Polyjet printing and extrusion printing are the most commonly used methods for 4D printing which both have some limitations, for example, polyjet printing has limited material choices, while extrusion-based printing suffers from slow printing speed and relatively low resolution.

6.3. Controlled Living Radical Photopolymerization.

Although 4D printing allows a 3D printed object to change its shape with time, the chemistry of free radical polymerization produces polymer products that are not “living”, which cannot be reinitiated to introduce new monomer/functionalities/

properties in a living manner. To design a living 3D printing approach, a highly efficient light-regulated controlled living radical polymerization is required. UV light-induced introduction of monomers into the formed polymer network has been experimentally investigated.^{201,202} For instance, a thermoresponsive *N*-isopropylacrylamide (NIPAAm) monomer was introduced into the strands of formed polymer networks containing trithiocarbonate (TTC) iniferters.²⁰¹ The solution homogeneous polymerization showed good evidence of living character; however, gel growth systems did not show living behaviors. This was due to the mechanism of UV-induced polymerization using chain transfer agents, which involves its photolysis to generate a propagating carbon-centered radical and an unstable TTC radical. In the gel growth system, light photons were mostly absorbed by the areas of the object close to the surface and underwent uncontrolled polymerization (decomposition) with no evidence of living chain growth throughout the entire network.²⁰¹ In a similar study, Kloxin and coworkers incorporated a dithiocarbamate iniferter within a polyurethane network to create a dynamic network with the ability to heal and strengthen. Under low intensity UV light irradiation, the carbon–sulfur bond of the incorporated dithiocarbamate iniferter could be cleaved to generate a radical and activate a free radical polymerization of the embedded dimethacrylate monomers. This results in an increase in the cross-link density and modulus of the materials. Although using the photoiniferter property of the chain transfer agents

was efficient to tune the network properties, the UV-induced photolysis mechanism is not controllable at the molecular level. This is in part due to the formation of unstable TTC radical intermediates with irreversible termination.²⁰²

An alternative approach is the use of a mechanism with different “reactive intermediates” such as a photoredox catalyzed RAFT polymerization, in which a photoredox catalyst activates RAFT polymerization via a photoinduced electron/energy transfer between the catalyst and the RAFT agent, allowing controlled living radical polymerization.^{41,137,203–208} Although photoredox catalyzed light-regulated polymerization technique has been utilized in a variety of contexts,^{155,209,210} its application in 3D printing has not been systematically explored. Only recently, Johnson and coworkers reported a proof-of-concept study of “living” 3D printing via photoredox catalyzed growth of uniform polymer gels.¹⁸ Parent gel networks bearing TTC iniferters were synthesized in the presence of a photocatalyst (10-phenylphenothiazine, PTH; 0.03% molar ratio of monomer) and monomer (such as NIPAAM, *n*-butyl acrylate or poly(ethylene glycol) methyl ether acrylate). The formed parent gel was then exposed to a blue LED light (410 nm) to excite PTH photocatalyst and hence activate photoinduced electron transfer to the network-conjugated TTC agent. The propagating strand can grow via a RAFT process; this means it can undergo degenerative chain transfer with nonactivated network-conjugated TTC. In the absence of light, the cleaved strands would reconnect, while back electron transfer to the photocatalyst radical cation occurs. This photoredox catalyzed RAFT process allows insertion of new monomer into the network in a living fashion. Depending on the monomers nature and cross-linker amount, daughter gels with different chemical and mechanical properties can be obtained from a parent gel (Figure 6).¹⁸ These findings can open a new way to fabricate 3D printed materials with living characters, however, more systematic studies is needed before it can be used in a 3D printer.²¹¹ In addition, the rate of controlled living radical polymerizations (such as photoredox catalyzed RAFT) is lower than the free radical polymerization, which might be a limiting factor to broaden the scope of its application in the 3D printing field with the need of fast build speed.

6.4. Tuning the Physicochemical and Mechanical Properties of the 3D Printed Materials. Photopolymerization-based techniques enable 3D fabrication of complex multifunctional materials with good control over the final properties required for various applications. One of the main drawbacks of the photopolymerization-based systems is the brittleness (poor impact resistance) due to the formation of inhomogeneous polymer network with high cross-link density. Strategies such as use of different forms of photopolymerization (i.e., thiol–ene chemistry (Section 3.1.2), use of AFCT (Section 3.1.3), or dual cure networks (Section 3.2)) can improve the molecular architecture of the polymer networks and enhance the mechanical properties of the 3D materials.⁵⁹ Besides these strategies with the focus on changing the chemistry of photopolymerization, efforts have been devoted to improve the toughness of the materials by addition of flexible oligomers into the photocurable resins.⁴⁸ For instance, addition of siloxane which has a semiorganic structure with excellent structural flexibility can change the reactivity, adhesion, surface energy, thermal stability, and also hydrophilicity of the 3D printed materials. Siloxanes have the tendency to move toward the lower surface tension (i.e., air),

which in the layer-by-layer nature of SLA process, this would result in the diffusion of siloxane to the surface of each layer and act as a filler in between the polymer matrix layers and therefore alter the roughness of the final printed materials. Advincula and coworkers reported the use of a liquid siloxane precursor (methacryloxypropyl methylsiloxane) combined with commercially available methacrylate oligomer to offer a siloxane-methacrylate photocurable resin.⁴⁸ Using a SLA-based 3D printing system (laser at 405 nm), 3D materials were produced with a decrease in the glass transition temperature value, surface energy, and tensile strength. In contrast, an increase in tensile toughness, ductility, compression break yield, and modulus was obtained.⁴⁸ Another study by the Advincula’s group showed that by addition of CNC into the PEGDA resin, 3D objects with improved mechanical and chemical properties can be obtained.²¹²

3D printed materials with high elasticity and stretchability are also desired for various applications.²¹³ In particular, elastomeric soft robotic systems require soft, elastic, flexible constituents to offer reasonable degrees of freedom and ability to exhibit large deformation. These properties would create a safe and smooth interaction with humans. Fabrication of soft robots is mostly obtained using “thermal” curable silicon rubber such as Ecoflex and Sylgard in a multistep molding and casting manufacturing approach, resulting in a limited geometric complexity.^{214,215} There are a few commercially available UV curable resins with elastomeric properties (Carbon EPU 40, Stratasys TangoPlus, Formlabs Flexible, and Spot-A Elastic) that can be used in SLA or DLP systems.³² However, these materials have certain limitations: (i) low value of the elongation at break (~170–220%) and (ii) fixed mechanical properties (Young’s modulus) obtained from commercial products than cannot be tuned.³² To tackle these issues, Magdassi and coworkers fabricated highly stretchable and UV curable (SUV) elastomer systems suitable for 3D printing process.³² A monofunctional monomer of epoxy aliphatic acrylate (EAA), a difunctional cross-linker (aliphatic urethane diacrylate (AUD)), and TPO were mixed to prepare the SUV elastomer resin. The addition of AUD which consists of soft compartment of aliphatic chains and hard compartment of urethane units offers flexibility. The modified SUV resin was photopolymerized using a DLP 3D printer (385 nm), which produced highly deformable and complex 3D structures (such as an isotropic truss structure and negative Poisson’s ratio structure).³² The stretchability of the printed elastomers (up to 1100%) was five times higher than the elongation at break of the commercial UV curable elastomers and comparable to the highly stretchable silicon rubber.³²

6.5. Shifting the Initiation Wavelength toward Longer Wavelengths. As elaborated in Section 4, the selection of excitation source is of critical practical importance to activate a photochemical reaction as chromophores are able to interact with photons of different wavelengths depending on their electronic configuration.²¹⁶ In early photopolymerization systems, photoinitiators with high molar extinction coefficients at short wavelength were used to initiate the photochemical pathway (Table 1).^{111,112} Although these photoinitiators offered good control over the photopolymerization systems, prolonged exposure to high energy wavelengths might result in side reactions with degradation of reactant and product. UV photons also present low penetration, and therefore, in the field of 3D printing, the accessible layer thicknesses usually

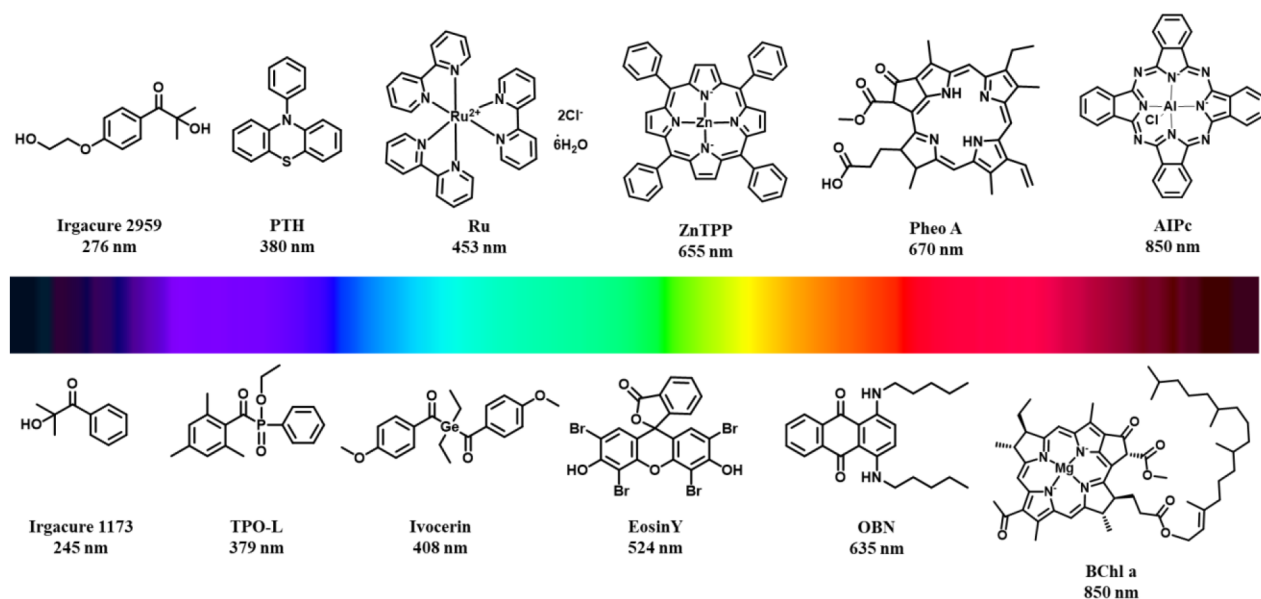


Figure 7. Examples of chromophores used as photoinitiator/photocatalysts in photopolymerization systems: oil blue N (OBN),²¹⁷ pheophorbide a (Pheo A),¹⁵⁵ bacteriochlorophyll a (BChl a),²¹⁸ and aluminum phthalocyanine (AlPc).²⁰⁸ Note 1: Some of these chromophores (such as ZnTPP) have multiple absorption peaks. Note 2: Some of these photoinitiators have been employed in 3D photopolymerization (refer to Tables 1 and 2) and are mentioned here for the sake of comparison.

remain low (below $\sim 100 \mu\text{m}$), resulting in a slow 3D printing rate (specifically for large objects).⁵⁴ Moreover, in the field of 3D bioprinting, the use of UV light also presents risk of cellular photodamage resulting in chromosomal and genetic instability in cells.¹² Therefore, development of photoinitiator systems with enhanced absorption in the longer irradiation wavelengths has been one of the main focuses of the 3D photopolymerization technologies with the aim of: (i) obtaining mild and safe condition of 3D printing, (ii) reaching higher penetration depth (layer thickness) resulting in enhancement in the photopolymerization rate, and (iii) providing a system that is benign to living cells for tissue engineering applications. Thus far, a number of photoinitiating systems with the ability to absorb in the visible range and initiate 3D photopolymerization have been investigated (Table 2). However, there are still plenty of possibilities for further innovative studies of 3D photopolymerization using previously established photoinitiators with absorbance in longer wavelength range (presented in Figure 7) or development of new photoinitiators/photocatalyst to drive the photochemical reactions in the 3D printing systems.

7. CONCLUSION

3D printing techniques based on photopolymerization such as SLA, DLP, and CLIP enable relatively fast and controlled construction of various architectures without the need for molds or machining. Using polymer chemistry-related innovations, 3D photopolymerization has opened new directions in various fields such as microfluidics, dentistry, biomedical devices, tissue engineering, and drug delivery. Nonetheless, despite its rapid growth, several challenges remain that limit its further progress. First, more diverse biocompatible materials with specific rheological, biological, mechanical, and chemical properties that can be used for 3D (or 4D) bioprinting application must be developed. In addition, 3D technologies with higher printing speed and resolution must be developed. Second, innovative studies are

required to produce 3D materials with living features that can be reinitiated to introduce new properties in a living manner. Third, the physicochemical and mechanical properties of the 3D printed materials must be further expanded by changing the chemistry of photopolymerization or use of additives to produce materials with desired properties. In addition, because 3D photopolymerization produces thermosets, more consideration on the degradability and recycling of the 3D printed objects is required to lessen the environmental contaminations. Fourthly, the development of photocurable formulations that can be photopolymerized under longer wavelengths irradiation is of considerable importance to obtain mild and safe condition of 3D photopolymerization while reaching higher penetration depth. Taken all together, this field is evolving at a very fast pace, and there is plenty of scope for further advanced studies. This extremely active research area requires multidisciplinary collaborative research, and it is expected to open new promises in numerous applications for industries.

AUTHOR INFORMATION

Corresponding Authors

*E-mail: Ali.bagheri@auckland.ac.nz.

*E-mail: j.jin@auckland.ac.nz.

ORCID

Ali Bagheri: [0000-0003-3484-5856](https://orcid.org/0000-0003-3484-5856)

Jianyong Jin: [0000-0002-5521-6277](https://orcid.org/0000-0002-5521-6277)

Notes

The authors declare no competing financial interest.

ACKNOWLEDGMENTS

J.J. and A.B. would like to thank the New Zealand Ministry of Business, Innovation and Employment (MBIE) Endeavour Fund for funding the Advanced Laser Microfabrication for NZ Industries research programme (UOAX-1701).

REFERENCES

- (1) Wendel, B.; Rietzel, D.; Kühnlein, F.; Feulner, R.; Hülber, G.; Schmachtenberg, E. Additive Processing of Polymers. *Macromol. Mater. Eng.* **2008**, *293*, 799–809.
- (2) Jungst, T.; Smolan, W.; Schacht, K.; Scheibel, T.; Groll, J. Strategies and Molecular Design Criteria for 3D Printable Hydrogels. *Chem. Rev.* **2016**, *116*, 1496–1539.
- (3) Layani, M.; Wang, X.; Magdassi, S. Novel Materials for 3D Printing by Photopolymerization. *Adv. Mater.* **2018**, *30*, 1–7.
- (4) Zhang, J.; Xiao, P. 3D Printing of Photopolymers. *Polym. Chem.* **2018**, *9*, 1530–1540.
- (5) Ligon, S. C.; Liska, R.; Stampfl, J.; Gurr, M.; Mülhaupt, R. Polymers for 3D Printing and Customized Additive Manufacturing. *Chem. Rev.* **2017**, *117*, 10212–10290.
- (6) Zarek, M.; Layani, M.; Cooperstein, I.; Sachyani, E.; Cohn, D.; Magdassi, S. 3D Printing of Shape Memory Polymers for Flexible Electronic Devices. *Adv. Mater.* **2016**, *28*, 4449–4454.
- (7) Wang, M. O.; Vorwald, C. E.; Dreher, M. L.; Mott, E. J.; Cheng, M. H.; Cinar, A.; Mehdizadeh, H.; Somo, S.; Dean, D.; Brey, E. M.; Fisher, J. P. Evaluating 3D-Printed Biomaterials as Scaffolds for Vascularized Bone Tissue Engineering. *Adv. Mater.* **2015**, *27*, 138–144.
- (8) Rusling, J. F. Developing Microfluidic Sensing Devices Using 3D Printing. *ACS Sensors* **2018**, *3*, 522–526.
- (9) Zorlutuna, P.; Jeong, J. H.; Kong, H.; Bashir, R. Stereolithography-Based Hydrogel Microenvironments to Examine Cellular Interactions. *Adv. Funct. Mater.* **2011**, *21*, 3642–3651.
- (10) Fu, J.; Yin, H.; Yu, X.; Xie, C.; Jiang, H.; Jin, Y.; Sheng, F. Combination of 3D Printing Technologies and Compressed Tablets for Preparation of Riboflavin Floating Tablet-in-Device (TiD) Systems. *Int. J. Pharm.* **2018**, *549*, 370–379.
- (11) Mondschein, R. J.; Kanitkar, A.; Williams, C. B.; Verbridge, S. S.; Long, T. E. Polymer Structure-Property Requirements for Stereolithographic 3D Printing of Soft Tissue Engineering Scaffolds. *Biomaterials* **2017**, *140*, 170–188.
- (12) Lim, K. S.; Schon, B. S.; Mekhileri, N. V.; Brown, G. C. J.; Chia, C. M.; Prabhakar, S.; Hooper, G. J.; Woodfield, T. B. F. New Visible-Light Photoinitiating System for Improved Print Fidelity in Gelatin-Based Bioinks. *ACS Biomater. Sci. Eng.* **2016**, *2*, 1752–1762.
- (13) Kabb, C. P.; O'Bryan, C. S.; Deng, C. C.; Angelini, T. E.; Sumerlin, B. S. Photoreversible Covalent Hydrogels for Soft-Matter Additive Manufacturing. *ACS Appl. Mater. Interfaces* **2018**, *10*, 16793–16801.
- (14) Zhang, J.; Dumur, F.; Xiao, P.; Graff, B.; Bardelang, D.; Gimes, D.; Fouassier, J. P.; Lalevée, J. Structure Design of Naphthalimide Derivatives: Toward Versatile Photoinitiators for Near-UV/Visible LEDs, 3D Printing, and Water-Soluble Photoinitiating Systems. *Macromolecules* **2015**, *48*, 2054–2063.
- (15) Juzenas, P.; Juzeniene, A.; Kaalhus, O.; Iani, V.; Moan, J. Noninvasive Fluorescence Excitation Spectroscopy during Application of 5-Aminolevulinic Acid in Vivo. *Photochem. Photobiol. Sci.* **2002**, *1*, 745–748.
- (16) Hudson, D. E.; Hudson, D. O.; Wining, J. M.; Richardson, B. D. Penetration of Laser Light at 808 and 980 Nm in Bovine Tissue Samples. *Photomed. Laser Surg.* **2013**, *31*, 163–168.
- (17) Rocheva, V. V.; Koroleva, A. V.; Savelyev, A. G.; Khaydukov, K. V.; Generalova, A. N.; Nechaev, A. V.; Guller, A. E.; Semchishen, V. A.; Chichkov, B. N.; Khaydukov, E. V. High-Resolution 3D Photopolymerization Assisted by Upconversion Nanoparticles for Rapid Prototyping Applications. *Sci. Rep.* **2018**, *8*, 1–10.
- (18) Chen, M.; Gu, Y.; Singh, A.; Zhong, M.; Jordan, A. M.; Biswas, S.; Korley, L. T. J.; Balazs, A. C.; Johnson, J. A. Living Additive Manufacturing: Transformation of Parent Gels into Diversely Functionalized Daughter Gels Made Possible by Visible Light Photoredox Catalysis. *ACS Cent. Sci.* **2017**, *3*, 124–134.
- (19) Rossi, S.; Puglisi, A.; Benaglia, M. Additive Manufacturing Technologies: 3D Printing in Organic Synthesis. *ChemCatChem* **2018**, *10*, 1512–1525.
- (20) Wu, G. H.; Hsu, S. H. Review: Polymeric-Based 3D Printing for Tissue Engineering. *J. Med. Biol. Eng.* **2015**, *35*, 285–292.
- (21) Tumbleston, J. R.; Shirvanyants, D.; Ermoshkin, N.; Januszewicz, R.; Johnson, A. R.; Kelly, D.; Chen, K.; Pinschmidt, R.; Rolland, J. P.; Ermoshkin, A.; Samulski, E. T.; DeSimone, J. M. Continuous Liquid Interface of 3D Objects. *Science* **2015**, *347*, 1349–1352.
- (22) Hull, C. W. Apparatus for Production of Three-Dimensional Objects by Stereolithography. U.S. Patent 4575330, 1986.
- (23) Hull, C. W.; Lewis, C. W. Methods and Apparatus for Production of Three-Dimensional Objects by Stereolithography. U.S. Patent 4999143, 1991.
- (24) Elomaa, L.; Pan, C. C.; Shanjani, Y.; Malkovskiy, A.; Seppälä, J. V.; Yang, Y. Three-Dimensional Fabrication of Cell-Laden Biodegradable Poly(Ethylene Glycol-Co-Depsipeptide) Hydrogels by Visible Light Stereolithography. *J. Mater. Chem. B* **2015**, *3*, 8348–8358.
- (25) Wang, X.; Jiang, M.; Zhou, Z.; Gou, J.; Hui, D. 3D Printing of Polymer Matrix Composites: A Review and Prospective. *Composites, Part B* **2017**, *110*, 442–458.
- (26) Palaganas, N. B.; Mangadla, J. D.; De Leon, A. C. C.; Palaganas, J. O.; Pangilinan, K. D.; Lee, Y. J.; Advincula, R. C. 3D Printing of Photocurable Cellulose Nanocrystal Composite for Fabrication of Complex Architectures via Stereolithography. *ACS Appl. Mater. Interfaces* **2017**, *9*, 34314–34324.
- (27) Credi, C.; Fiorese, A.; Tironi, M.; Bernasconi, R.; Magagnin, L.; Levi, M.; Turri, S. 3D Printing of Cantilever-Type Microstructures by Stereolithography of Ferromagnetic Photopolymers. *ACS Appl. Mater. Interfaces* **2016**, *8*, 26332–26342.
- (28) Zhu, W.; Qu, X.; Zhu, J.; Ma, X.; Patel, S.; Liu, J.; Wang, P.; Lai, C. S. E.; Gou, M.; Xu, Y.; Zhang, K.; Chen, S. Direct 3D Bioprinting of Prevascularized Tissue Constructs with Complex Microarchitecture. *Biomaterials* **2017**, *124*, 106–115.
- (29) Soman, P.; Chung, P. H.; Zhang, A. P.; Chen, S. Digital Microfabrication of User-Defined 3D Microstructures in Cell-Laden Hydrogels. *Biotechnol. Bioeng.* **2013**, *110*, 3038–3047.
- (30) De Leon, A. C.; Chen, Q.; Palaganas, N. B.; Palaganas, J. O.; Manapat, J.; Advincula, R. C. High Performance Polymer Nanocomposites for Additive Manufacturing Applications. *React. Funct. Polym.* **2016**, *103*, 141–155.
- (31) Wang, F.; Chong, Y.; Wang, F. K.; He, C. Photopolymer Resins for Luminescent Three-Dimensional Printing. *J. Appl. Polym. Sci.* **2017**, *134*, 1–8.
- (32) Patel, D. K.; Sakhaei, A. H.; Layani, M.; Zhang, B.; Ge, Q.; Magdassi, S. Highly Stretchable and UV Curable Elastomers for Digital Light Processing Based 3D Printing. *Adv. Mater.* **2017**, *29*, 1–7.
- (33) Zhu, W.; Tringale, K. R.; Woller, S. A.; You, S.; Johnson, S.; Shen, H.; Schimelman, J.; Whitney, M.; Steinauer, J.; Xu, W.; Yaksh, T. L.; Nguyen, Q. T.; Chen, S. Rapid Continuous 3D Printing of Customizable Peripheral Nerve Guidance Conduits. *Mater. Today* **2018**, *21*, 951–959.
- (34) Zhang, B.; Kowsari, K.; Serjouei, A.; Dunn, M. L.; Ge, Q. Reprocessable Thermosets for Sustainable Three-Dimensional Printing. *Nat. Commun.* **2018**, *9*, 1831.
- (35) Mu, Q.; Wang, L.; Dunn, C. K.; Kuang, X.; Duan, F.; Zhang, Z.; Qi, H. J.; Wang, T. Digital Light Processing 3D Printing of Conductive Complex Structures. *Addit. Manuf.* **2017**, *18*, 74–83.
- (36) Cullen, A. T.; Price, A. D. Digital Light Processing for the Fabrication of 3D Intrinsically Conductive Polymer Structures. *Synth. Met.* **2018**, *235*, 34–41.
- (37) Chiappone, A.; Fantino, E.; Roppolo, I.; Lorusso, M.; Manfredi, D.; Fino, P.; Pirri, C. F.; Calignano, F. 3D Printed PEG-Based Hybrid Nanocomposites Obtained by Sol–Gel Technique. *ACS Appl. Mater. Interfaces* **2016**, *8*, 5627–5633.
- (38) Wang, J.; Stanic, S.; Altun, A. A.; Schwentenwein, M.; Dietliker, K.; Jin, L.; Stampfl, J.; Baudis, S.; Liska, R.; Grützmaier, H. A Highly Efficient Waterborne Photoinitiator for Visible-Light-Induced Three-

Dimensional Printing of Hydrogels. *Chem. Commun.* **2018**, *54*, 920–923.

(39) Dilla, R. A.; Motta, C. M. M.; Snyder, S. R.; Wilson, J. A.; Wesdemiotis, C.; Becker, M. L. Synthesis and 3D Printing of PEG–Poly(Propylene Fumarate) Diblock and Triblock Copolymer Hydrogels. *ACS Macro Lett.* **2018**, *7*, 1254–1260.

(40) Oesterreicher, A.; Wiener, J.; Roth, M.; Moser, A.; Gmeiner, R.; Edler, M.; Pinter, G.; Griesser, T. Tough and Degradable Photopolymers Derived from Alkyne Monomers for 3D Printing of Biomedical Materials. *Polym. Chem.* **2016**, *7*, 5169–5180.

(41) Xu, J.; Jung, K.; Atme, A.; Shanmugam, S.; Boyer, C. A Robust and Versatile Photoinduced Living Polymerization of Conjugated and Unconjugated Monomers and Its Oxygen Tolerance. *J. Am. Chem. Soc.* **2014**, *136*, 5508–5519.

(42) Desimone, J. M.; Samulski, E. T.; Ermoshkin, A.; DeSimone, P. M. Rapid 3D Continuous Printing of Casting Molds for Metals and Other Materials. *Int. Patent Appl. WO2015080888*, 2015.

(43) Januszewicz, R.; Tumbleston, J. R.; Quintanilla, A. L.; Mecham, S. J.; DeSimone, J. M. Layerless Fabrication with Continuous Liquid Interface Production. *Proc. Natl. Acad. Sci. U. S. A.* **2016**, *113*, 11703–11708.

(44) Fouassier, J. P.; Allonas, X.; Lalevée, J.; Dietlin, C. Photoinitiators for Free Radical Polymerization Reactions. In *Photochemistry and Photophysics of Polymer Materials*; Allen, N. S., Ed.; John Wiley & Sons, 2010; p i-712.

(45) Jasinski, F.; Zetterlund, P. B.; Braun, A. M.; Chemtob, A. Photopolymerization in Dispersed Systems. *Prog. Polym. Sci.* **2018**, *84*, 47–88.

(46) Wayner, D. D. M.; Clark, K. B.; Rauk, A.; Yu, D.; Armstrong, D. A. C-H Bond Dissociation Energies of Alkyl Amines: Radical Structures and Stabilisation Energies. *J. Am. Chem. Soc.* **1997**, *119*, 8925–8932.

(47) Zheng, X.; Smith, W.; Jackson, J.; Moran, B.; Cui, H.; Chen, D.; Ye, J.; Fang, N.; Rodriguez, N.; Weisgraber, T.; Spadaccini, C. M. Multiscale Metallic Metamaterials. *Nat. Mater.* **2016**, *15*, 1100–1106.

(48) Palaganas, J.; de Leon, A. C.; Mangalao, J.; Palaganas, N.; Mael, A.; Lee, Y. J.; Lai, H. Y.; Advincula, R. Facile Preparation of Photocurable Siloxane Composite for 3D Printing. *Macromol. Mater. Eng.* **2017**, *302* (5), 1–9.

(49) Stassi, S.; Fantino, E.; Calmo, R.; Chiappone, A.; Gillono, M.; Scaiola, D.; Pirri, C. F.; Ricciardi, C.; Chiadò, A.; Roppolo, I. Polymeric 3D Printed Functional Microcantilevers for Biosensing Applications. *ACS Appl. Mater. Interfaces* **2017**, *9* (22), 19193–19201.

(50) Gou, M.; Qu, X.; Zhu, W.; Xiang, M.; Yang, J.; Zhang, K.; Wei, Y.; Chen, S. Bio-Inspired Detoxification Using 3D-Printed Hydrogel Nanocomposites. *Nat. Commun.* **2014**, *5*, 3774.

(51) Warner, J.; Soman, P.; Zhu, W.; Tom, M.; Chen, S. Design and 3D Printing of Hydrogel Scaffolds with Fractal Geometries. *ACS Biomater. Sci. Eng.* **2016**, *2*, 1763–1770.

(52) Liska, R.; Schuster, M.; Inführ, R.; Turecek, C.; Fritscher, C.; Seidl, B.; Schmidt, V.; Kuna, L.; Haase, A.; Varga, F.; Lichtenegger, H.; Stampfl, J. Photopolymers for Rapid Prototyping. *J. Coatings Technol. Res.* **2007**, *4*, 505–510.

(53) Yue, J.; Zhao, P.; Gerasimov, J. Y.; Van De Lagemaat, M.; Grotenhuis, A.; Rustema-Abbing, M.; Van Der Mei, H. C.; Busscher, H. J.; Herrmann, A.; Ren, Y. 3D-Printable Antimicrobial Composite Resins. *Adv. Funct. Mater.* **2015**, *25*, 6756–6767.

(54) Al Mousawi, A.; Garra, P.; Sallenave, X.; Dumur, F.; Toufaily, J.; Hamieh, T.; Graff, B.; Gignes, D.; Fouassier, J. P.; Lalevée, J. π Conjugated Dithienophosphole Derivatives as High Performance Photoinitiators for 3D Printing Resins. *Macromolecules* **2018**, *51*, 1811–1821.

(55) Al Mousawi, A.; Kermagoret, A.; Versace, D. L.; Toufaily, J.; Hamieh, T.; Graff, B.; Dumur, F.; Gignes, D.; Fouassier, J. P.; Lalevée, J. Copper Photoredox Catalysts for Polymerization upon near UV or Visible Light: Structure/Reactivity/Efficiency Relationships and Use in LED Projector 3D Printing Resins. *Polym. Chem.* **2017**, *8*, 568–580.

(56) Al Mousawi, A.; Dumur, F.; Garra, P.; Toufaily, J.; Hamieh, T.; Graff, B.; Gignes, D.; Fouassier, J. P.; Lalevée, J. Carbazole Scaffold Based Photoinitiator/Photoredox Catalysts: Toward New High Performance Photoinitiating Systems and Application in LED Projector 3D Printing Resins. *Macromolecules* **2017**, *50*, 2747–2758.

(57) Al Mousawi, A.; Garra, P.; Schmitt, M.; Toufaily, J.; Hamieh, T.; Graff, B.; Fouassier, J. P.; Dumur, F.; Lalevée, J. 3-Hydroxyflavone and N-Phenylglycine in High Performance Photoinitiating Systems for 3D Printing and Photocomposites Synthesis. *Macromolecules* **2018**, *51*, 4633–4641.

(58) Boddapati, A.; Rahane, S. B.; Slopek, R. P.; Breedveld, V.; Henderson, C. L.; Grover, M. A. Gel Time Prediction of Multifunctional Acrylates Using a Kinetics Model. *Polymer* **2011**, *52*, 866–873.

(59) Ligon-Auer, S. C.; Schwentenwein, M.; Gorsche, C.; Stampfl, J.; Liska, R. Toughening of Photo-Curable Polymer Networks: A Review. *Polym. Chem.* **2016**, *7*, 257–286.

(60) Kim, L. U.; Kim, J. W.; Kim, C. K. Effects of Molecular Structure of the Resins on the Volumetric Shrinkage and the Mechanical Strength of Dental Restorative Composites. *Biomacromolecules* **2006**, *7*, 2680–2687.

(61) Hull, C. W.; Spence, S. T.; Lewis, C. W.; Vinson, W.; Freed, R. S.; Smalley, D. R. Stereolithographic Curl Reduction. U.S. Patent 5772947, 1998.

(62) Moraes, R. R.; Garcia, J. W.; Barros, M. D.; Lewis, S. H.; Pfeifer, C. S.; Liu, J.; Stansbury, J. W. Control of Polymerization Shrinkage and Stress in Nanogel-Modified Monomer and Composite Materials. *Dent. Mater.* **2011**, *27*, 509–519.

(63) Lovestead, T. M.; O'Brien, A. K.; Bowman, C. N. Models of Multivinyl Free Radical Photopolymerization Kinetics. *J. Photochem. Photobiol., A* **2003**, *159*, 135–143.

(64) Moad, G.; Rizzardo, E.; Thang, S. H. Radical Addition-Fragmentation Chemistry in Polymer Synthesis. *Polymer* **2008**, *49*, 1079–1131.

(65) Gorsche, C.; Seidler, K.; Knaack, P.; Dorfinger, P.; Koch, T.; Stampfl, J.; Moszner, N.; Liska, R. Rapid Formation of Regulated Methacrylate Networks Yielding Tough Materials for Lithography-Based 3D Printing. *Polym. Chem.* **2016**, *7*, 2009–2014.

(66) Yagci, Y.; Jockusch, S.; Turro, N. J. Photoinitiated Polymerization: Advances, Challenges, and Opportunities. *Macromolecules* **2010**, *43*, 6245–6260.

(67) Mirlle, S. K.; Kumpfmiller, R. J. Photosensitive Compositions Useful in Three-Dimensional Part-Building and Having Improved Photospeed. U.S. Patent 5418112, 1995.

(68) Decker, C.; Viet, T. N. T.; Decker, D. UV-Radiation Curing of Acrylate/Epoxy Systems. *Polymer* **2001**, *42*, 5531–5541.

(69) Steinmann, B. Stereolithographic Resins with High Temperature and High Impact Resistance. U.S. Patent 6989225, 2006.

(70) Ganster, B.; Fischer, U. K.; Moszner, N.; Liska, R. New Photocleavable Structures. Diacylgermane-based Photoinitiators for Visible Light Curing. *Macromolecules* **2008**, *41*, 2394–2400.

(71) Hoyle, C. E.; Bowman, C. N. Thiol-Ene Click Chemistry. *Angew. Chem., Int. Ed.* **2010**, *49*, 1540–1573.

(72) Kade, M. J.; Burke, D. J.; Hawker, C. J. The Power of Thiol ene Chemistry. *J. Polym. Sci., Part A: Polym. Chem.* **2010**, *48*, 743–750.

(73) Hoyle, C. E.; Lee, T. Y.; Roper, T. Thiol-Ene: Chemistry of the Past with Promise for the Future. *J. Polym. Sci., Part A: Polym. Chem.* **2004**, *42*, 5301–5338.

(74) Husár, B.; Ligon, S. C.; Wutzel, H.; Hoffmann, H.; Liska, R. The Formulator's Guide to Anti-Oxygen Inhibition Additives. *Prog. Org. Coat.* **2014**, *77*, 1789–1798.

(75) McNair, O. D.; Janisse, A. P.; Krzeminski, D. E.; Brent, D. E.; Gould, T. E.; Rawlins, J. W.; Savin, D. A. Impact Properties of Thiol-Ene Networks. *ACS Appl. Mater. Interfaces* **2013**, *5*, 11004–11013.

(76) Qin, X. H.; Gruber, P.; Markovic, M.; Plochberger, B.; Klotzsch, E.; Stampfl, J.; Ovsianikov, A.; Liska, R. Enzymatic Synthesis of Hyaluronic Acid Vinyl Esters for Two-Photon Microfabrication of Biocompatible and Biodegradable Hydrogel Constructs. *Polym. Chem.* **2014**, *5*, 6523–6533.

- (77) Bertlein, S.; Brown, G.; Lim, K. S.; Jungst, T.; Boeck, T.; Blunk, T.; Tessmar, J.; Hooper, G. J.; Woodfield, T. B. F.; Groll, J. Thiol-Ene Clickable Gelatin: A Platform Bioink for Multiple 3D Biofabrication Technologies. *Adv. Mater.* **2017**, *29*, 1–6.
- (78) Kumpfmüller, J.; Stadlmann, K.; Li, Z.; Satzinger, V.; Stampfl, J.; Liska, R. Two-Photon-Induced Thiol-Ene Polymerization as a Fabrication Tool for Flexible Optical Waveguides. *Des. Monomers Polym.* **2014**, *17*, 390–400.
- (79) Quick, A. S.; Fischer, J.; Richter, B.; Paulohrl, T.; Trouillet, V.; Wegener, M.; Barner-Kowollik, C. Preparation of Reactive Three-Dimensional Microstructures via Direct Laser Writing and Thiol-Ene Chemistry. *Macromol. Rapid Commun.* **2013**, *34*, 335–340.
- (80) Senyurt, A. F.; Wei, H.; Phillips, B.; Cole, M.; Nazarenko, S.; Hoyle, C. E.; Piland, S. G.; Gould, T. E. Physical and Mechanical Properties of Photopolymerized Thiol-Ene/Acrylates. *Macromolecules* **2006**, *39*, 6315–6317.
- (81) Sycks, D. G.; Wu, T.; Park, H. S.; Gall, K. Tough, Stable Spiroacetal Thiol-Ene Resin for 3D Printing. *J. Appl. Polym. Sci.* **2018**, *135*, 1–12.
- (82) Mongkhontreerat, S.; Öberg, K.; Erixon, L.; Löwenhielm, P.; Hult, A.; Malkoch, M. UV Initiated Thiol-Ene Chemistry: A Facile and Modular Synthetic Methodology for the Construction of Functional 3D Networks with Tunable Properties. *J. Mater. Chem. A* **2013**, *1*, 13732–13737.
- (83) Chen, L.; Wu, Q.; Wei, G.; Liu, R.; Li, Z. Highly Stable Thiol-Ene System: From Structure-Property Relationship to DLP 3D Printing. *J. Mater. Chem. C* **2018**, *6*, 11561–11568.
- (84) Senyurt, A. F.; Hoyle, C. E.; Wei, H.; Piland, S. G.; Gould, T. E. Thermal and Mechanical Properties of Cross-Linked Photopolymers Based on Multifunctional Thiol-Urethane Ene Monomers. *Macromolecules* **2007**, *40*, 3174–3182.
- (85) Dias, A. J. A. A.; Houben, E. J. E.; Steeman, P. A. M.; Wei, H. Radiation Curable Thiol-Ene Composition. Eur. Patent App. EP1477511 A1, 2004.
- (86) Esfandiari, P.; Ligon, S. C.; Lagref, J. J.; Frantz, R.; Cherkaoui, Z.; Liska, R. Efficient Stabilization of Thiol-Ene Formulations in Radical Photopolymerization. *J. Polym. Sci., Part A: Polym. Chem.* **2013**, *51*, 4261–4266.
- (87) Belbakra, Z.; Cherkaoui, Z. M.; Allonas, X. Photocurable Polythiol Based (Meth)Acrylate Resins Stabilization: New Powerful Stabilizers and Stabilization Systems. *Polym. Degrad. Stab.* **2014**, *110*, 298–307.
- (88) Fairbanks, B. D.; Sims, E. A.; Anseth, K. S.; Bowman, C. N. Reaction Rates and Mechanisms for Radical, Photoinitiated Addition of Thiols to Alkynes, and Implications for Thiol-Yne Photopolymerizations and Click Reactions. *Macromolecules* **2010**, *43*, 4113–4119.
- (89) Chan, J. W.; Shin, J.; Hoyle, C. E.; Bowman, C. N.; Lowe, A. B. Synthesis, Thiol-Yne “Click” Photopolymerization, and Physical Properties of Networks Derived from Novel Multifunctional Alkynes. *Macromolecules* **2010**, *43*, 4937–4942.
- (90) Scott, T. F. Photoinduced Plasticity in Cross-Linked Polymers. *Science* **2005**, *308*, 1615–1617.
- (91) Blasco, E.; Wegener, M.; Barner-Kowollik, C. Photochemically Driven Polymeric Network Formation: Synthesis and Applications. *Adv. Mater.* **2017**, *29*, 1604005.
- (92) Gorsche, C.; Griesser, M.; Gescheidt, G.; Moszner, N.; Liska, R. β -Allyl Sulfones as Addition-Fragmentation Chain Transfer Reagents: A Tool for Adjusting Thermal and Mechanical Properties of Dimethacrylate Networks. *Macromolecules* **2014**, *47*, 7327–7336.
- (93) Gorsche, C.; Koch, T.; Moszner, N.; Liska, R. Exploring the Benefits of β -Allyl Sulfones for More Homogeneous Dimethacrylate Photopolymer Networks. *Polym. Chem.* **2015**, *6*, 2038–2047.
- (94) Crivello, J. V. The Discovery and Development Of. *J. Polym. Sci., Part A: Polym. Chem.* **1999**, *37*, 4241–4254.
- (95) Crivello, J. V.; Lam, J. H. W. Photoinitiated Cationic Polymerization with Triarylsulfonium Salts. *J. Polym. Sci., Part A: Polym. Chem.* **1996**, *34*, 3231–3253.
- (96) Matsumura, S.; Hlil, A. R.; Lepiller, C.; Gaudet, J.; Guay, D.; Shi, Z.; Holdcroft, S.; Hay, A. S. Ionomers for Proton Exchange Membrane Fuel Cells with Sulfonic Acid Groups on the End-Groups: Novel Branched Poly(Ether-Ketone)S. *Macromolecules* **2008**, *41*, 281–284.
- (97) Crivello, J. V.; Lam, J. H. W. Complex Triarylsulfonium Salt Photoinitiators. I. The Identification, Characterization, and Syntheses of a New Class of Triarylsulfonium Salt Photoinitiators. *J. Polym. Sci., Polym. Chem. Ed.* **1980**, *18*, 2677–2695.
- (98) Al Mousawi, A.; Poriel, C.; Dumur, F.; Toufaily, J.; Hamieh, T.; Fouassier, J. P.; Lalevée, J. Zinc Tetraphenylporphyrin as High Performance Visible Light Photoinitiator of Cationic Photosensitive Resins for LED Projector 3D Printing Applications. *Macromolecules* **2017**, *50*, 746–753.
- (99) Steinmann, B.; Schulthess, A. Liquid, Radiation-Curable Composition, Especially for Stereolithography. U.S. Patent 5972563, 1999.
- (100) Al Mousawi, A.; Dumur, F.; Garra, P.; Toufaily, J.; Hamieh, T.; Goubard, F.; Bui, T. T.; Graff, B.; Gignes, D.; Pierre Fouassier, J.; Lalevée, J. Azahelicenes as Visible Light Photoinitiators for Cationic and Radical Polymerization: Preparation of Photoluminescent Polymers and Use in High Performance LED Projector 3D Printing Resins. *J. Polym. Sci., Part A: Polym. Chem.* **2017**, *55*, 1189–1199.
- (101) Zhang, J.; Dumur, F.; Xiao, P.; Graff, B.; Gignes, D.; Pierre Fouassier, J.; Lalevée, J. Aminothiazonaphthalic Anhydride Derivatives as Photoinitiators for Violet/Blue LED-Induced Cationic and Radical Photopolymerizations and 3D-Printing Resins. *J. Polym. Sci., Part A: Polym. Chem.* **2016**, *54*, 1189–1196.
- (102) Al Mousawi, A.; Lara, D. M.; Noirbent, G.; Dumur, F.; Toufaily, J.; Hamieh, T.; Bui, T. T.; Goubard, F.; Graff, B.; Gignes, D.; Fouassier, J. P.; Lalevée, J. Carbazole Derivatives with Thermally Activated Delayed Fluorescence Property as Photoinitiators/Photo-redox Catalysts for LED 3D Printing Technology. *Macromolecules* **2017**, *50*, 4913–4926.
- (103) Steinmann, B.; Wolf, J.; Schulthess, A.; Hunziker, M. Photosensitive Compositions. U.S. Patent 5476748, 1995.
- (104) Lapim, S. C.; Snyder, J. R.; Sitzmann, E. V.; Barnes, D. K.; Green, G. D. Stereolithography Using Vinyl Ether-Epoxy Polymers. U.S. Patent 5437964, 1995.
- (105) Xu, J. Photo-Curable Resin Composition. U.S. Patent 9090020, 2015.
- (106) Yamamura, T.; Watanabe, T.; Takeuchi, A.; Ukachi, T. Photo-Curable Resin Composition Used for Photo Fabrication of Three-Dimensional Objects. U.S. Patent 5981616, 1997.
- (107) Lapim, S. C.; Brautigam, R. J. Stereolithography Using Vinyl Ether Based Polymers. U.S. Patent 5506087, 1996.
- (108) Xiao, P.; Dumur, F.; Frigoli, M.; Tehfe, M. A.; Graff, B.; Fouassier, J. P.; Gignes, D.; Lalevée, J. Naphthalimide Based Methacrylated Photoinitiators in Radical and Cationic Photopolymerization under Visible Light. *Polym. Chem.* **2013**, *4*, 5440–5448.
- (109) Ohkawa, K. A. D. K. K.; Saito, S. A. D. K. K. Resin Composition for Optical Modeling. Eur. Patent App. EP 0360869, 1990.
- (110) Cai, Y.; Jessop, J. L. P. Decreased Oxygen Inhibition in Photopolymerized Acrylate/Epoxy Hybrid Polymer Coatings as Demonstrated by Raman Spectroscopy. *Polymer* **2006**, *47*, 6560–6566.
- (111) Lalevée, J.; Tehfe, M. A.; Dumur, F.; Gignes, D.; Graff, B.; Morlet-Savary, F.; Fouassier, J. P. Light-Harvesting Organic Photoinitiators of Polymerization. *Macromol. Rapid Commun.* **2013**, *34*, 239–245.
- (112) Wiersma, D. The Smallest Random Laser. *Nature* **2000**, *406*, 133–135.
- (113) Fouassier, J. P.; Allonas, X.; Burget, D. Photopolymerization Reactions under Visible Lights: Principle, Mechanisms and Examples of Applications. *Prog. Org. Coat.* **2003**, *47* (1), 16–36.
- (114) Ravve, A. *Light-Associated Reactions of Synthetic Polymers*; Springer: New York, 2006; p i-369.

- (115) Schafer, K. J.; Hales, J. M.; Balu, M.; Belfield, K. D.; Van Stryland, E. W.; Hagan, D. J. Two-Photon Absorption Cross-Sections of Common Photoinitiators. *J. Photochem. Photobiol., A* **2004**, *162*, 497–502.
- (116) Fantino, E.; Chiappone, A.; Calignano, F.; Fontana, M.; Pirri, F.; Roppolo, I. In Situ Thermal Generation of Silver Nanoparticles in 3D Printed Polymeric Structures. *Materials* **2016**, *9*, 21–23.
- (117) Chan, V.; Zorlutuna, P.; Jeong, J. H.; Kong, H.; Bashir, R. Three-Dimensional Photopatterning of Hydrogels Using Stereolithography for Long-Term Cell Encapsulation. *Lab Chip* **2010**, *10*, 2062–2070.
- (118) Chan, V.; Jeong, J. H.; Bajaj, P.; Collens, M.; Saif, T.; Kong, H.; Bashir, R. Multi-Material Bio-Fabrication of Hydrogel Cantilevers and Actuators with Stereolithography. *Lab Chip* **2012**, *12*, 88–98.
- (119) Occhetta, P.; Visone, R.; Russo, L.; Cipolla, L.; Moretti, M.; Rasponi, M. VA-086 Methacrylate Gelatine Photopolymerizable Hydrogels: A Parametric Study for Highly Biocompatible 3D Cell Embedding. *J. Biomed. Mater. Res., Part A* **2015**, *103*, 2109–2117.
- (120) Rouillard, A. D.; Berglund, C. M.; Lee, J. Y.; Polachek, W. J.; Tsui, Y.; Bonassar, L. J.; Kirby, B. J. Methods for Photocrosslinking Alginate Hydrogel Scaffolds with High Cell Viability. *Tissue Eng., Part C* **2011**, *17*, 173–179.
- (121) Chandler, E. M.; Berglund, C. M.; Lee, J. S.; Polachek, W. J.; Gleghorn, J. P.; Kirby, B. J.; Fischbach, C. Stiffness of Photocrosslinked RGD-Alginate Gels Regulates Adipose Progenitor Cell Behavior. *Biotechnol. Bioeng.* **2011**, *108*, 1683–1692.
- (122) Lin, H.; Zhang, D.; Alexander, P. G.; Yang, G.; Tan, J.; Cheng, A. W. M.; Tuan, R. S. Application of Visible Light-Based Projection Stereolithography for Live Cell-Scaffold Fabrication with Designed Architecture. *Biomaterials* **2013**, *34*, 331–339.
- (123) Manojlovic, D.; Dramićanin, M. D.; Lezaja, M.; Pongprueksa, P.; Van Meerbeek, B.; Miletic, V. Effect of Resin and Photoinitiator on Color, Translucency and Color Stability of Conventional and Low-Shrinkage Model Composites. *Dent. Mater.* **2016**, *32*, 183–191.
- (124) Park, H. K.; Shin, M.; Kim, B.; Park, J. W.; Lee, H. A Visible Light-Curable yet Visible Wavelength-Transparent Resin for Stereolithography 3D Printing. *NPG Asia Mater.* **2018**, *10*, 82–89.
- (125) Basu, M.; Sarkar, S.; Pande, S.; Jana, S.; Kumar Sinha, A.; Sarkar, S.; Pradhan, M.; Pal, A.; Pal, T. Hydroxylation of Benzophenone with Ammonium Phosphomolybdate in the Solid State via UV Photoactivation. *Chem. Commun.* **2009**, *46*, 7191–7193.
- (126) Melhem, M. R.; Park, J.; Knapp, L.; Reinkensmeyer, L.; Cvetkovic, C.; Flewellyn, J.; Lee, M. K.; Jensen, T. W.; Bashir, R.; Kong, H.; Schook, L. B. 3D Printed Stem-Cell-Laden, Microchanneled Hydrogel Patch for the Enhanced Release of Cell-Secreting Factors and Treatment of Myocardial Infarctions. *ACS Biomater. Sci. Eng.* **2017**, *3*, 1980–1987.
- (127) Williams, C. G.; Malik, A. N.; Kim, T. K.; Manson, P. N.; Elisseff, J. H. Variable Cytocompatibility of Six Cell Lines with Photoinitiators Used for Polymerizing Hydrogels and Cell Encapsulation. *Biomaterials* **2005**, *26*, 1211–1218.
- (128) Gauvin, R.; Chen, Y. C.; Lee, J. W.; Soman, P.; Zorlutuna, P.; Nichol, J. W.; Bae, H.; Chen, S.; Khademhosseini, A. Microfabrication of Complex Porous Tissue Engineering Scaffolds Using 3D Projection Stereolithography. *Biomaterials* **2012**, *33*, 3824–3834.
- (129) Mann, B. K.; Gobin, A. S.; Tsai, A. T.; Schmedlen, R. H.; West, J. L. Smooth Muscle Cell Growth in Photopolymerized Hydrogels with Cell Adhesive and Proteolytically Degradable Domains: Synthetic ECM Analogs for Tissue Engineering. *Biomaterials* **2001**, *22*, 3045–3051.
- (130) Vatani, M.; Choi, J. W. Direct-Print Photopolymerization for 3D Printing. *Rapid Prototyp. J.* **2017**, *23*, 337–343.
- (131) Zhu, W.; Li, J.; Leong, Y. J.; Rozen, I.; Qu, X.; Dong, R.; Wu, Z.; Gao, W.; Chung, P. H.; Wang, J.; Chen, S. 3D-Printed Artificial Microfish. *Adv. Mater.* **2015**, *27*, 4411–4417.
- (132) Qu, X.; Zhu, W.; Huang, S.; Li, Y. S.; Chien, S.; Zhang, K.; Chen, S. Relative Impact of Uniaxial Alignment vs. Form-Induced Stress on Differentiation of Human Adipose Derived Stem Cells. *Biomaterials* **2013**, *34*, 9812–9818.
- (133) Fairbanks, B.; Schwartz, M.; Bowman, C.; Anseth, K. Photoinitiated Polymerisation of PEG-Diacrylate with Lithium Phenyl-2,4,6-Trimethylbenzoylphosphinate: Polymerisation Rate and Cytocompatibility. *Biomaterials* **2009**, *30*, 6702–6707.
- (134) Huang, T. Q.; Qu, X.; Liu, J.; Chen, S. 3D Printing of Biomimetic Microstructures for Cancer Cell Migration. *Biomed. Microdevices* **2014**, *16*, 127–132.
- (135) van Bochove, B.; Hannink, G.; Buma, P.; Grijpma, D. W. Preparation of Designed Poly(Trimethylene Carbonate) Meniscus Implants by Stereolithography: Challenges in Stereolithography. *Macromol. Biosci.* **2016**, *16*, 1853–1863.
- (136) Fors, B. P.; Hawker, C. J. Control of a Living Radical Polymerization of Methacrylates by Light. *Angew. Chem., Int. Ed.* **2012**, *51*, 8850–8853.
- (137) Xu, J.; Shanmugam, S.; Duong, H. T.; Boyer, C. Organo-Photocatalysts for Photoinduced Electron Transfer-Reversible Addition-Fragmentation Chain Transfer (PET-RAFT) Polymerization. *Polym. Chem.* **2015**, *6*, 5615–5624.
- (138) Bagheri, A.; Arandiyani, H.; Adnan, N. N. M.; Boyer, C.; Lim, M. Controlled Direct Growth of Polymer Shell on Upconversion Nanoparticle Surface via Visible Light Regulated Polymerization. *Macromolecules* **2017**, *50*, 7137–7147.
- (139) Sadrearhami, Z.; Yeow, J.; Nguyen, T.; Ho, K. K. K.; Kumar, N.; Boyer, C. Biofilm Dispersal Using Nitric Oxide Loaded Nanoparticles Fabricated by Photo-PISA: Influence of Morphology. *Chem. Commun.* **2017**, *53*, 12894–12897.
- (140) Bagheri, A.; Arandiyani, H.; Boyer, C.; Lim, M. Lanthanide-Doped Upconversion Nanoparticles: Emerging Intelligent Light-Activated Drug Delivery Systems. *Adv. Sci.* **2016**, *3*, 1500437.
- (141) Jauk, S.; Liska, R. Photoinitiators with Functional Groups. *Macromol. Rapid Commun.* **2005**, *26*, 1687–1692.
- (142) Steyrer, B.; Neubauer, P.; Liska, R.; Stampfl, J. Visible Light Photoinitiator for 3D-Printing of Tough Methacrylate Resins. *Materials* **2017**, *10*, 1–11.
- (143) Xiao, P.; Dumur, F.; Graff, B.; Gimes, D.; Fouassier, J. P.; Lalevée, J. Blue Light Sensitive Dyes for Various Photopolymerization Reactions: Naphthalimide and Naphthalic Anhydride Derivatives. *Macromolecules* **2014**, *47*, 601–608.
- (144) Corrigan, N.; Shanmugam, S.; Xu, J.; Boyer, C. Photocatalysis in Organic and Polymer Synthesis. *Chem. Soc. Rev.* **2016**, *45*, 6165–6212.
- (145) Ohtsuki, A.; Goto, A.; Kaji, H. Visible-Light-Induced Reversible Complexation Mediated Living Radical Polymerization of Methacrylates with Organic Catalysts. *Macromolecules* **2013**, *46*, 96–102.
- (146) Pham, P. V.; Nagib, D. A.; MacMillan, D. W. C. Photoredox Catalysis: A Mild, Operationally Simple Approach to the Synthesis of α -Trifluoromethyl Carbonyl Compounds. *Angew. Chem., Int. Ed.* **2011**, *50*, 6119–6122.
- (147) Nicewicz, D. A.; MacMillan, D. W. C. Merging Photoredox Catalysis with Organocatalysis: The Direct Asymmetric Alkylation of Aldehydes. *Science* **2008**, *322*, 77–80.
- (148) Zeitler, K. Photoredox Catalysis with Visible Light. *Angew. Chem., Int. Ed.* **2009**, *48*, 9785–9789.
- (149) Dadashi-Silab, S.; Doran, S.; Yagci, Y. Photoinduced Electron Transfer Reactions for Macromolecular Syntheses. *Chem. Rev.* **2016**, *116*, 10212–10275.
- (150) Konkolewicz, D.; Schroder, K.; Buback, J.; Bernhard, S.; Matyjaszewski, K. Visible Light and Sunlight Photoinduced ATRP with Ppm of Cu Catalyst. *ACS Macro Lett.* **2012**, *1*, 1219–1223.
- (151) Xu, J.; Jung, K.; Boyer, C. Oxygen Tolerance Study of Photoinduced Electron Transfer–Reversible Addition–Fragmentation Chain Transfer (PET-RAFT) Polymerization Mediated by Ru(Bpy)₃Cl₂. *Macromolecules* **2014**, *47*, 4217–4229.
- (152) Hill, M. R.; Carmean, R. N.; Sumerlin, B. S. Expanding the Scope of RAFT Polymerization: Recent Advances and New Horizons. *Macromolecules* **2015**, *48*, 5459–5469.

- (153) Murtezi, E.; Yagci, Y. Simultaneous Photoinduced ATRP and CuAAC Reactions for the Synthesis of Block Copolymers. *Macromol. Rapid Commun.* **2014**, *35*, 1782–1787.
- (154) Xiao, P.; Dumur, F.; Zhang, J.; Fouassier, J. P.; Gignes, D.; Lalevée, J. Copper Complexes in Radical Photoinitiating Systems: Applications to Free Radical and Cationic Polymerization upon Visible Leds. *Macromolecules* **2014**, *47*, 3837–3844.
- (155) Bagheri, A.; Yeow, J.; Arandiyana, H.; Xu, J.; Boyer, C.; Lim, M. Polymerization of a Photocleavable Monomer Using Visible Light. *Macromol. Rapid Commun.* **2016**, *37*, 905–910.
- (156) Bagheri, A.; Sadreahami, Z.; Adnan, N. N. M.; Boyer, C.; Lim, M. Surface Functionalization of Upconversion Nanoparticles Using Visible Light-Mediated Polymerization. *Polymer* **2018**, *151*, 6–14.
- (157) Matyjaszewski, K.; Tsarevsky, N. V. Macromolecular Engineering by Atom Transfer Radical Polymerization. *J. Am. Chem. Soc.* **2014**, *136*, 6513–6533.
- (158) Xu, J.; Sivaprakash, S.; Nathaniel Alan, C.; Cyrille, B. Catalyst-Free Visible Light-Induced RAFT Photopolymerization. In *Controlled Radical Polymerization: Mechanisms*; ACS Symposium Series eBooks; American Chemical Society, 2015; p i–339.
- (159) Huang, Z.; Gu, Y.; Liu, X.; Zhang, L.; Cheng, Z.; Zhu, X. Metal-Free Atom Transfer Radical Polymerization of Methyl Methacrylate with Ppm Level of Organic Photocatalyst. *Macromol. Rapid Commun.* **2017**, *38*, 1–8.
- (160) Zanchetta, E.; Cattaldo, M.; Franchin, G.; Schwentenwein, M.; Homa, J.; Brusatin, G.; Colombo, P. Stereolithography of SiOC Ceramic Microcomponents. *Adv. Mater.* **2016**, *28*, 370–376.
- (161) Lee, D.-H.; Mai, H. N.; Yang, J.-C.; Kwon, T.-Y. The Effect of 4,4'-Bis(N,N-Diethylamino) Benzophenone on the Degree of Conversion in Liquid Photopolymer for Dental 3D Printing. *J. Adv. Prosthodont.* **2015**, *7*, 386–391.
- (162) Erskine, L. L.; Heikal, A. a.; Kuebler, S. M.; Rumi, M.; Wu, X.; Marder, S. R.; Perry, J. W. Two-Photon Polymerization Initiators for Three-Dimensional Optical Data Storage and Microfabrication. *Solid State Phys.* **1999**, *398*, 51–54.
- (163) Mayer, J. G. Über Elementarakte Mit Zwei Quantensprungen. *Ann. Phys.* **1931**, *401*, 273–294.
- (164) Juodkazis, S.; Mizeikis, V.; Seet, K. K.; Miwa, M.; Misawa, H. Two-Photon Lithography of Nanorods in SU-8 Photoresist. *Nanotechnology* **2005**, *16*, 846–849.
- (165) Xing, J.; Zheng, M.; Duan, X. Two-Photon Polymerization Microfabrication of Hydrogels: An Advanced 3D Printing Technology for Tissue Engineering and Drug Delivery. *Chem. Soc. Rev.* **2015**, *44*, 5031–5039.
- (166) Ovsianikov, A.; Mironov, V.; Stampfl, J.; Liska, R.; Ovsianikov, A.; Mironov, V. Engineering 3D Cell-Culture Matrices: Multiphoton Processing Technologies for Biological and Tissue Engineering Applications. *Expert Rev. Med. Devices* **2012**, *9*, 613–633.
- (167) Pawlicki, M.; Collins, H. A.; Denning, R. G.; Anderson, H. L. Two-Photon Absorption and the Design of Two-Photon Dyes. *Angew. Chem., Int. Ed.* **2009**, *48*, 3244–3266.
- (168) Whitby, R.; Ben-Tal, Y.; MacMillan, R.; Janssens, S.; Raymond, S.; Clarke, D.; Jin, J.; Kay, A.; Simpson, M. C. Photoinitiators for Two-Photon Polymerisation: Effect of Branching and Viscosity on Polymerisation Thresholds. *RSC Adv.* **2017**, *7*, 13232–13239.
- (169) Bagheri, A.; Li, Z.; Boyer, C.; Lim, M. NIR/Blue Light Emission Optimization of NaY_{1-(x+y)}Yb_xF₄:Tm_y Upconversion Nanoparticles via Yb³⁺/Tm³⁺ Dopant Balancing. *Dalt. Trans.* **2018**, *47*, 8629–8637.
- (170) Yin, A.; Zhang, Y.; Sun, L.; Yan, C. Colloidal Synthesis and Blue Based Multicolor Upconversion Emissions of Size and Composition Controlled Monodisperse Hexagonal NaYF₄Yb,Tm Nanocrystals. *Nanoscale* **2010**, *2*, 953–959.
- (171) Ding, C.; Wang, J.; Zhang, W.; Pan, X.; Zhang, Z.; Zhang, W.; Zhu, J.; Zhu, X. Platform of Near-Infrared Light-Induced Reversible Deactivation Radical Polymerization: Upconversion Nanoparticles as Internal Light Sources. *Polym. Chem.* **2016**, *7*, 7370–7374.
- (172) Liu, R.; Chen, H.; Li, Z.; Shi, F.; Liu, X. Extremely Deep Photopolymerization Using Upconversion Particles as Internal Lamps. *Polym. Chem.* **2016**, *7*, 2457–2463.
- (173) Beyazit, S.; Ambrosini, S.; Marchyk, N.; Palo, E.; Kale, V.; Soukka, T.; Tse Sum Bui, B.; Haupt, K. Versatile Synthetic Strategy for Coating Upconverting Nanoparticles with Polymer Shells through Localized Photopolymerization by Using the Particles as Internal Light Sources. *Angew. Chem., Int. Ed.* **2014**, *53*, 8919–8923.
- (174) Chai, R.; Lian, H.; Cheng, Z.; Zhang, C.; Hou, Z.; Xu, Z.; Lin, J. Preparation and Characterization of Upconversion Luminescent NaYF₄Yb, Er (Tm)/PS Bulk Transparent Nanocomposites through In Situ Polymerization. *J. Colloid Interface Sci.* **2010**, *345*, 262–268.
- (175) Darani, M. K.; Bastani, S.; Ghahari, M.; Kardar, P.; Mohajerani, E. NIR Induced Photopolymerization of Acrylate-Based Composite Containing Upconversion Particles as an Internal Miniaturized UV Sources. *Prog. Org. Coat.* **2017**, *104*, 97–103.
- (176) Xie, Z.; Deng, X.; Liu, B.; Huang, S.; Ma, P.; Hou, Z.; Cheng, Z.; Lin, J.; Luan, S. Construction of Hierarchical Polymer Brushes on Upconversion Nanoparticles via NIR-Light-Initiated RAFT Polymerization. *ACS Appl. Mater. Interfaces* **2017**, *9*, 30414–30425.
- (177) Stepuk, A.; Mohn, D.; Grass, R. N.; Zehnder, M.; Krämer, K. W.; Pellé, F.; Ferrier, A.; Stark, W. J. Use of NIR Light and Upconversion Phosphors in Light-Curable Polymers. *Dent. Mater.* **2012**, *28*, 304–311.
- (178) Méndez-Ramos, J.; Ruiz-Morales, J. C.; Acosta-Mora, P.; Khaidukov, N. M. Infrared-Light Induced Curing of Photosensitive Resins through Photon up-Conversion for Novel Cost-Effective Luminescent 3D-Printing Technology. *J. Mater. Chem. C* **2016**, *4*, 801–806.
- (179) Panzer, M.; Tumbleston, J. R. Continuous Liquid Interface Production with Upconversion Photopolymerization U. S. Patent 20180126630 A1, 2018.
- (180) Ozbolat, I. T.; Hospodiuk, M. Current Advances and Future Perspectives in Extrusion-Based Bioprinting. *Biomaterials* **2016**, *76*, 321–343.
- (181) Ouyang, L.; Highley, C. B.; Sun, W.; Burdick, J. A. A Generalizable Strategy for the 3D Bioprinting of Hydrogels from Nonviscous Photo-Crosslinkable Inks. *Adv. Mater.* **2017**, *29*, 1604983.
- (182) O'Bryan, C. S.; Bhattacharjee, T.; Marshall, S. L.; Gregory Sawyer, W.; Angelini, T. E. Commercially Available Microgels for 3D Bioprinting. *Bioprinting* **2018**, *11*, No. e00037.
- (183) Andrews, L. S.; Clary, J. J. Review of the Toxicity of Multifunctional Acrylates. *J. Toxicol. Environ. Health* **1986**, *19*, 149–164.
- (184) Mautner, A.; Qin, X.; Kapeller, B.; Russmueller, G.; Koch, T.; Stampfl, J.; Liska, R. Efficient Curing of Vinyl Carbonates by Thiol-Ene Polymerization. *Macromol. Rapid Commun.* **2012**, *33*, 2046–2052.
- (185) Soman, P.; Fozdar, D. Y.; Lee, J. W.; Phadke, A.; Varghese, S.; Chen, S. A Three-Dimensional Polymer Scaffolding Material Exhibiting a Zero Poisson's Ratio. *Soft Matter* **2012**, *8*, 4946–4951.
- (186) Tibbitt, M. W.; Anseth, K. S. Hydrogels as Extracellular Matrix Mimics for 3D Cell Culture. *Biotechnol. Bioeng.* **2009**, *103*, 655–663.
- (187) Gong, H.; Beauchamp, M.; Perry, S.; Woolley, A. T.; Nordin, G. P. Optical Approach to Resin Formulation for 3D Printed Microfluidics. *RSC Adv.* **2015**, *5*, 106621–106632.
- (188) Mu, X.; Bertron, T.; Dunn, C.; Qiao, H.; Wu, J.; Zhao, Z.; Saldana, C.; Qi, H. J. Porous Polymeric Materials by 3D Printing of Photocurable Resin. *Mater. Horiz.* **2017**, *4*, 442–449.
- (189) Wang, J.; Goyanes, A.; Gaisford, S.; Basit, A. W. Stereolithographic (SLA) 3D Printing of Oral Modified-Release Dosage Forms. *Int. J. Pharm.* **2016**, *503*, 207–212.
- (190) Ma, X.; Qu, X.; Zhu, W.; Li, Y.-S.; Yuan, S.; Zhang, H.; Liu, J.; Wang, P.; Lai, C. S. E.; Zanella, F.; Feng, G. S. Deterministically Patterned Biomimetic Human iPSC-Derived Hepatic Model via Rapid 3D Bioprinting. *Proc. Natl. Acad. Sci. U. S. A.* **2016**, *113*, 2206–2211.

- (191) Kuang, X.; Roach, D. J.; Wu, J.; Hamel, C. M.; Ding, Z.; Wang, T.; Dunn, M. L.; Qi, H. J. Advances in 4D Printing: Materials and Applications. *Adv. Funct. Mater.* **2019**, *29*, 1805290.
- (192) Lee, J.; Kim, H. C.; Choi, J. W.; Lee, I. H. A Review on 3D Printed Smart Devices for 4D Printing. *Int. J. Precis. Eng. Manuf. - Green Technol.* **2017**, *4*, 373–383.
- (193) Sydney Gladman, A.; Matsumoto, E. A.; Nuzzo, R. G.; Mahadevan, L.; Lewis, J. A. Biomimetic 4D Printing. *Nat. Mater.* **2016**, *15*, 413–418.
- (194) Momeni, F.; Mehdi Hassani, S. M.; Liu, X.; Ni, J. A Review of 4D Printing. *Mater. Des.* **2017**, *122*, 42–79.
- (195) Yang, H.; Leow, W. R.; Wang, T.; Wang, J.; Yu, J.; He, K.; Qi, D.; Wan, C.; Chen, X. 3D Printed Photoresponsive Devices Based on Shape Memory Composites. *Adv. Mater.* **2017**, *29*, 1701627.
- (196) Kotikian, A.; Truby, R. L.; Boley, J. W.; White, T. J.; Lewis, J. A. 3D Printing of Liquid Crystal Elastomeric Actuators with Spatially Programed Nematic Order. *Adv. Mater.* **2018**, *30* (10), 1706164.
- (197) Dutta, S.; Cohn, D. Temperature and PH Responsive 3D Printed Scaffolds. *J. Mater. Chem. B* **2017**, *5*, 9514–9521.
- (198) Roppolo, I.; Chiappone, A.; Angelini, A.; Stassi, S.; Frascella, F.; Pirri, C. F.; Ricciardi, C.; Descrovi, E. 3D Printable Light-Responsive Polymers. *Mater. Horiz.* **2017**, *4*, 396–401.
- (199) Zhao, Z.; Kuang, X.; Yuan, C.; Qi, H. J.; Fang, D. Hydrophilic/Hydrophobic Composite Shape-Shifting Structures. *ACS Appl. Mater. Interfaces* **2018**, *10*, 19932–19939.
- (200) Gao, B.; Yang, Q.; Zhao, X.; Jin, G.; Ma, Y.; Xu, F. 4D Bioprinting for Biomedical Applications. *Trends Biotechnol.* **2016**, *34*, 746–756.
- (201) Zhou, H.; Johnson, J. A. Photo-Controlled Growth of Telechelic Polymers and End-Linked Polymer Gels. *Angew. Chem., Int. Ed.* **2013**, *52*, 2235–2238.
- (202) Gordon, M. B.; French, J. M.; Wagner, N. J.; Kloxin, C. J. Dynamic Bonds in Covalently Crosslinked Polymer Networks for Photoactivated Strengthening and Healing. *Adv. Mater.* **2015**, *27*, 8007–8010.
- (203) Xu, J.; Shanmugam, S.; Boyer, C. Organic Electron Donor-Acceptor Photoredox Catalysts: Enhanced Catalytic Efficiency toward Controlled Radical Polymerization. *ACS Macro Lett.* **2015**, *4*, 926–932.
- (204) Niu, J.; Lunn, D. J.; Pusuluri, A.; Yoo, J. I.; O'Malley, M. A.; Mitragotri, S.; Soh, H. T.; Hawker, C. J. Engineering Live Cell Surfaces with Functional Polymers via Cytocompatible Controlled Radical Polymerization. *Nat. Chem.* **2017**, *9*, 537–545.
- (205) Tucker, B. S.; Coughlin, M. L.; Figg, C. A.; Sumerlin, B. S. Grafting-From Proteins Using Metal-Free PET-RAFT Polymerizations under Mild Visible-Light Irradiation. *ACS Macro Lett.* **2017**, *6*, 452–457.
- (206) Shanmugam, S.; Xu, J.; Boyer, C. Exploiting Metalloporphyrins for Selective Living Radical Polymerization Tunable over Visible Wavelengths. *J. Am. Chem. Soc.* **2015**, *137*, 9174–9185.
- (207) Ng, G.; Yeow, J.; Xu, J.; Boyer, C. Application of Oxygen Tolerant PET-RAFT to Polymerization-Induced Self-Assembly. *Polym. Chem.* **2017**, *8*, 2841–2851.
- (208) Corrigan, N.; Xu, J.; Boyer, C. A Photoinitiation System for Conventional and Controlled Radical Polymerization at Visible and NIR Wavelengths. *Macromolecules* **2016**, *49*, 3274–3285.
- (209) Chen, M.; MacLeod, M. J.; Johnson, J. A. Visible-Light-Controlled Living Radical Polymerization from a Trithiocarbonate Iniferter Mediated by an Organic Photoredox Catalyst. *ACS Macro Lett.* **2015**, *4*, 566–569.
- (210) Miyake, G. M.; Theriot, J. C. Perylene as an Organic Photocatalyst for the Radical Polymerization of Functionalized Vinyl Monomers through Oxidative Quenching with Alkyl Bromides and Visible Light. *Macromolecules* **2014**, *47*, 8255–8261.
- (211) Shanmugam, S.; Xu, J.; Boyer, C. Living Additive Manufacturing. *ACS Cent. Sci.* **2017**, *3*, 95–96.
- (212) Yang, J.; Han, C. R.; Duan, J. F.; Xu, F.; Sun, R. C. Mechanical and Viscoelastic Properties of Cellulose Nanocrystals Reinforced Poly(Ethylene Glycol) Nanocomposite Hydrogels. *ACS Appl. Mater. Interfaces* **2013**, *5*, 3199–3207.
- (213) Mosadegh, B.; Polygerinos, P.; Keplinger, C.; Wennstedt, S.; Shepherd, R. F.; Gupta, U.; Shim, J.; Bertoldi, K.; Walsh, C. J.; Whitesides, G. M. Pneumatic Networks for Soft Robotics That Actuate Rapidly. *Adv. Funct. Mater.* **2014**, *24*, 2163–2170.
- (214) Tolley, M. T.; Shepherd, R. F.; Mosadegh, B.; Galloway, K. C.; Wehner, M.; Karpelson, M.; Wood, R. J.; Whitesides, G. M. A Resilient, Untethered Soft Robot. *Soft Robot.* **2014**, *1*, 213–223.
- (215) Muth, J. T.; Vogt, D. M.; Truby, R. L.; Mengüç, Y.; Kolesky, D. B.; Wood, R. J.; Lewis, J. A. Embedded 3D Printing of Strain Sensors within Highly Stretchable Elastomers. *Adv. Mater.* **2014**, *26*, 6307–6312.
- (216) Lu, L.; Zhang, H.; Yang, N.; Cai, Y. Toward Rapid and Well-Controlled Ambient Temperature RAFT Polymerization under UV - Vis Radiation: Effect of Radiation Wave Range. *Macromolecules* **2006**, *39*, 3770–3776.
- (217) Xiao, P.; Dumur, F.; Graff, B.; Fouassier, J. P.; Gimes, D.; Lalevée, J. Cationic and Thiol-Ene Photopolymerization upon Red Lights Using Anthraquinone Derivatives as Photoinitiators. *Macromolecules* **2013**, *46*, 6744–6750.
- (218) Shanmugam, S.; Xu, J.; Boyer, C. Light-Regulated Polymerization under Near-Infrared/Far-Red Irradiation Catalyzed by Bacteriochlorophyll A. *Angew. Chem., Int. Ed.* **2016**, *55*, 1036–1040.